On the Performance of Cognitive Satellite-Terrestrial Networks

Citation for published version:
Kolawole, O, Vuppala, S, Sellathurai, M & Ratnarajah, T 2017, 'On the Performance of Cognitive Satellite-Terrestrial Networks', *IEEE Transactions on Cognitive Communications and Networking*, vol. 3, no. 4, pp. 668 - 683. https://doi.org/10.1109/TCCN.2017.2763619

Digital Object Identifier (DOI):
10.1109/TCCN.2017.2763619

Published In:
IEEE Transactions on Cognitive Communications and Networking

On the Performance of Cognitive Satellite-Terrestrial Networks

Oluwatayo Y. Kolawole, *Student Member, IEEE*, Satyanarayana Vuppala, *Member, IEEE*, Mathini Sellathurai, *Senior Member, IEEE*, and Tharmalingam Ratnarajah, *Senior Member, IEEE*

AQ1

***Abstract*—We investigate the performance of a multi-beam cognitive satellite terrestrial network in which a secondary network (mobile terrestrial system) shares resources with a primary satellite network given that the interference temperature constraint is satisfied. The terrestrial base stations (BSs) and satellite users are modeled as independent homogeneous Poisson point processes. Utilizing tools from stochastic geometry, we study and compare the outage performance of three secondary transmission schemes: first is the power constraint (PCI) scheme where the transmit power at the terrestrial BS is limited by the interference temperature constraint. In the second scheme, the terrestrial BSs employ directional beamforming to focus the signal intended for the terrestrial user, and in the third, BSs that do not satisfy the interference temperature constraint are thinned out (BTPI). Analytical approximations of all three schemes are derived and validated through numerical simulations. It is shown that for the least interference to the satellite user, BTPI is the best scheme. However, when thinning is not feasible, PCI scheme is the viable alternative. In addition, the gains of directional beamforming are optimal when the terrestrial system employs massive multiple-input-multiple-output transceivers or by the use of millimeter wave links between terrestrial BSs and users.**

***Index Terms*—Cognitive radio, interference, multi-beam satellite, poisson point processes, satellite-terrestrial networks.**

I. Introduction

THE KEY goals of future generation wireless communication systems include billions of connected devices, data rates in the range of Gbps, lower latencies, increased reliability, improved coverage and environment-friendly, low-cost, and energy-efficient operation. As the existing cellular spectrum approaches its performance limits, there is growing interest in and exploration of supplementary resources for meeting these demands [1]. As a result, satellite mobile communication is attracting widespread interest in radio technology studies which aim to provide ample coverage with low complexity infrastructure [2]. Multi-beam structure in modern satellite mobile communication has gained massive attention because of the potential to provide a higher coverage area and larger capacity since multiple isolated spot beams can reuse frequency. For example, with a reuse factor of four, hundreds of beams are possible [3]. The frequency reuse in multi-beam satellites gives a trade-off between inter-beam interference and available bandwidth as presented in [4]. Precoding techniques have been established to increase communication efficiency [1]. In the context of multi-beam satellites, precoding techniques are being explored as a means to mitigate inter-beam interference. The work in [5] shows that with the use of linear precoding, spectral efficiency is improved by about fifty percent. Moreover, motivated by the advances in cellular communication to improve spectral efficiency, hybrid satellite-terrestrial networks have gained interest in research [6], [7].

Cognitive radio is another technology that has attracted considerable research as a means of spectrum management in conventional wireless communication systems because it allows the coexistence of primary and secondary networks using the same resources [8], [9]. A primary network consists of transmitters and receivers with the licence to use a specific frequency band [10] while a secondary network comprises the transmitters and receivers that share resources with the primary network. Cognitive radio networks operate three major paradigms: underlay, overlay and interweave [9]. Within the framework of satellite communication, Sharma *et al.* [11] suggest that the level of interference power can determine which cognitive technique is appropriate. The underlay paradigm, which allows concurrent primary (non-cognitive) and secondary (cognitive) transmissions, and is suitable for medium interference regions, is considered in this paper.

In addition, the fusion of cognitive radios with hybrid satellite-terrestrial networks (cognitive satellite-terrestrial networks, CSTNs) is investigated by many researchers with the objective of optimizing efficiency and coverage in both existing and future wireless communication systems.

Manuscript received March 30, 2017; revised July 20, 2017 and October 3, 2017; accepted October 4, 2017. The work of O. Kolawole was supported by the PTDF agency of the Federal government of Nigeria with the mandate to build capacities and capabilities in Nigeria's Oil and Gas Industry through the development of human capacities and promotion of research and acquisition of relevant technologies, the work of S. Vuppala, and T. Ratnarajah was supported by the U.K. Engineering and Physical Sciences Research Council (EPSRC) under grants EP/L025299/1, and the work of M. Sellathurai was funded by EPSRC Project EP/M014126/1, Large Scale Antenna Systems Made Practical: Advanced Signal Processing for Compact Deployments. The associate editor coordinating the review of this paper and approving it for publication was N. Devroye. *(Corresponding author: Oluwatayo Y. Kolawole.)*

AQ2

O. Kolawole and T. Ratnarajah are with the Institute for Digital Communications, University of Edinburgh, Edinburgh EH9 3JL, U.K. (e-mail: o.kolawole@ed.ac.uk; t.ratnarajah@ed.ac.uk).

S. Vuppala was with the Institute for Digital Communications, University of Edinburgh, Edinburgh EH9 3JL, U.K. He is now with the Interdisciplinary Centre for Security, Reliability and Trust, University of Luxembourg, 1855 Luxembourg City, Luxembourg (e-mail: satyanarayana.vuppala@uni.lu).

M. Sellathurai is with the Department of Electrical, Electronic and Computer Engineering, Herriot-Watt University, Edinburgh EH14 4AS, U.K. (e-mail: m.sellathurai@hw.ac.uk).

Digital Object Identifier 10.1109/TCCN.2017.2763619

The work in [12] introduced the concept to show the possibility of maximising spectrum utilization for terrestrial ground and satellite uplink transmissions. Additional works enhancing CSTNs include [13]–[16]. Specifically, the work in [13] presents methods for utilizing underlay CSTNs, power allocation is considered in [14] and performance of CSTNs under imperfect channel estimations is measured using the metrics of outage probability and normalised capacity. Lagunas *et al.* [15] investigate efficient allocation of more resources such as carrier, power and bandwidth allocations for achieving more gain with the CSTNs, and finally, the work in [16] presents a mathematical approach to achieve computational efficiency of the outage probability of CSTNs.

With the incorporation of base stations (BSs) to satellite communication, terrestrial interference is another key parameter that needs to be characterized for the accurate analysis of the performance of CSTNs. Given the random locations of terrestrial BSs as well as satellite users [17] and motivated by the successes of using stochastic geometry models for interference characterization in cellular cognitive radio networks [18], [19], we employ the probabilistic stochastic geometric tools for characterizing the interference in CSTNs.

To achieve performance gains, numerous studies have sought ways of managing interference. A well known method for this management is directional transmission [20], [21], which focuses a signal to a target direction (unlike the omni-directional method in which a signal is transmitted in all directions). Directional transmission has the advantage of reducing interference and increasing coverage. In CSTNs, Sharma *et al.* [22] study different beamforming techniques to jointly achieve maximum rate for the secondary user and minimize interference to the satellite users and show that modified linear constrained minimum variance beamformer achieves this objective.

A. Design Approaches

This paper evaluates the performance of a CSTN where there is concurrent transmission of a primary multi-beam satellite network and a secondary terrestrial mobile network, and where interference to the primary network is not beyond a set limit. We provide a comparative analysis of different methods for keeping interference generated by the terrestrial network within acceptable limits.

In [13]–[16], all nodes are assumed to be equipped with a single antenna. However, in the proposed CSTN model, the nodes of the secondary (terrestrial) network will be equipped with multiple antennas as well as multiple beams considered for the satellite network. Therefore, unlike the models in [13]–[16], this work considers a more general and practical scenario with the analysis of a network where multiple terrestrial base stations (BSs) share resources with a multi-beamed satellite to serve the terrestrial user. To the authors' best knowledge, randomly distributed BS with multiple antennas has not been considered for this network set-up.

Introducing multiple BSs with multiple antennas at the secondary network results in a more involved analysis than is presented in [13]–[16], because apart from characterizing the strict interference constraints imposed by the satellite network, there is an added interference from other terrestrial BSs trying to serve the terrestrial user. In this paper therefore, we characterize this added interference by using stochastic geometric tools, and consider its effect on the transmissions in both primary and secondary networks.

The performance of this network is analysed for three different transmission schemes. In the first, we assume that the BS process of the secondary network is stationary and ergodic so that BS nodes take part in transmission to the terrestrial user only if they satisfy the interference temperature constraint imposed by the satellite. Thus, we design a framework for characterizing the transmission power at the BS to ensure that the interference limit imposed by the primary network is not surpassed, and also characterize the interference by the BSs that do not satisfy the constraint. This scheme is referred to as power constraint to limit interference (PCI). In the second (DBI), we utilize directional transmission at the secondary system to focus the signals intended for the terrestrial user and accordingly restrict interference to acceptable limits. This scheme is based on the interference limit and thus no power restriction is placed on the terrestrial BSs. Finally, because some BSs may not participate in transmission owing to their inability to satisfy this interference temperature constraint, we will consider for the third scheme only the subset of BSs that meet the satellite's requirement. This consideration leads to a marked point process and will be referred to as the BS thinning process to restrict interference (BTPI). It is important to note that the thinning criteria is based on transmit power constraint which will be described in Section II.

The performance of these schemes are analysed in terms of outage probability at both satellite and terrestrial users. To gain further insight, we also study the area spectral efficiency of the secondary system in order to investigate the impact of interference temperature on the average number of successful transmitted symbols. The analysis presented here adds valuable insights to recent works on CSTNs.

B. Contributions

The main contributions of the paper can be summarized as follows:

- We have presented a more general model of CSTN where a multi-beam satellite shares resources with randomly distributed BSs (equipped with multiple antennas) as long as the interference temperature constraint imposed by the satellite system is satisfied.
- We have presented analysis of this network under three schemes of limiting interference generated by the secondary system.
  - Power constraint to limit interference (PCI): in this method, the only participating BSs are those that satisfy the primary systems requirements. This requirement is satisfied by restricting the transmit power at the BSs.
  - Directional beamforming to control interference (DBI): here, a transmitting BS utilizes directional beamforming to focus the intended signal to the user,

thus restricting interference to the primary network within required limits.
  - BS thinning process to restrict interference (BTPI): the assumption in this method is that not all BSs would satisfy the constraint set by the primary network. These non-satisfying BSs are thinned out so that only the subset of BSs that satisfy the constraint participate in communication.
- To analyse the performance of this network, we introduce two important metrics: *outage probability* to measure the effect of interference from BSs other than the intended BS on both satellite and terrestrial communication, and *area spectral efficiency* to investigate the impact of interference temperature on spectrum efficiency at the secondary system.
- We also provide a detailed analysis on the effect of channel fading, BS node density and signal-to-interference-plus-noise ratio (SINR) threshold on a CSTN.
- Via numerical results, we show the effective trade-off between outage probability performance and number of antennas at each BS and terrestrial user. In addition, BTPI is the best scheme of secondary transmission in a CSTN because of its strict adherence to the satellite system's requirements thereby producing least interference to the satellite user of the three schemes. Finally, where thinning is not feasible, for a conventional terrestrial mobile system, restricting the transmit power at the terrestrial BS (PCI) is the viable option.

Notations: We use upper and lower case to denote cumulative distribution functions (CDFs) and probability density functions (PDFs) respectively. $\mathbb{R}$ denotes the real plane, Probability is denoted by $\mathcal{P}$, expectation by $\mathbb{E}[\,\cdot\,]$, and $\exp(\cdot)$ and $e^{(\cdot)}$ are used interchangeably to represent the exponential function, and all other symbols will be explicitly defined wherever used.

The rest of the paper is organized as follows. Section II describes the system model. The transmission characterization of multi-beam CSTN is presented in Section III. Section IV gives the numerical analysis, followed by the conclusion in Section V.

II. System Model

We consider the downlink of a multi-beam CSTN consisting of a satellite whose coverage area is served by K spot beams (known as the primary system) and terrestrial BSs sharing resources with the satellite to communicate with a terrestrial user (secondary system) as shown in fig. 1. h_{pp} and h_{cc} represent the direct channel links from the satellite and a given BS to their respective users, while h_{pc} and h_{cp} are the interference links from satellite to terrestrial user and from BS to satellite user respectively.

In the primary system, the satellite transmits to users using K beams. The users are geographically scattered from which a cluster of K beams are formed. Without loss of generality, a single feed per beam is assumed. Thus, each beam is paired with a single user at a given instance. To manage interference between adjacent beams and reduce the round trip

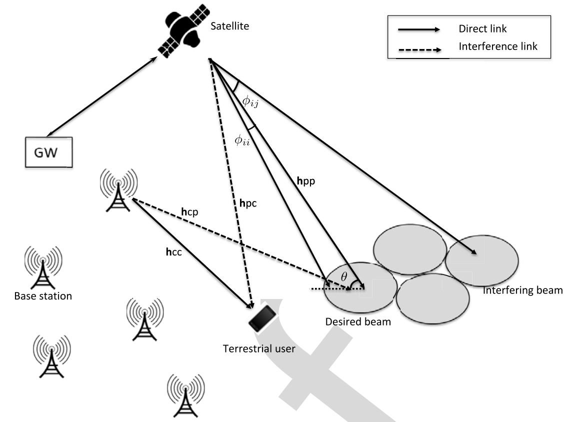

Fig. 1. An illustration of network set-up. AQ3

delays, multiple gateways (GWs) have been proposed to manage clusters of beams so that distributed joint processing can be utilized [23]. However, in this paper we focus on a single gateway (GW) which manages a cluster of K beams with an ideal link between satellite and GW. It is assumed that perfect channel state information is obtainable at the GW[1]; these assumptions are typical in [3], [17], and [24].[2] To reduce the expense of backhauling, joint processing is performed at the GW so that each of K user's signal is jointly precoded and transmitted across all beams [3]. In addition, zero-forcing (ZF) precoder for interference management between beams is considered.[3]

In the secondary system, the underlay cognitive paradigm is employed which allows the terrestrial BSs to transmit concurrently with the satellite as long as interference to the primary user is below a certain threshold.

A. Network Model

In this section, we illustrate our system model of a downlink multi-beam CSTN consisting of multiple satellite users with terrestrial BSs serving their desired user. The satellite users in the network are modelled as points in $\mathbb{R}^2$ which are distributed uniformly in the beam radius as a homogeneous Poisson point process (PPP), Φ_U with intensity λ_U as illustrated in Fig. 2. We assume that a cluster of K beams is formed of users geographically close together, in other words, the users in a Voronoi cell comprise a cluster resulting in a coverage area that make up a Voronoi tessellation on the plane. Hence, the total number of beams, K, can be determined with the help of λ_U. The BSs are also modelled as points of a uniform PPP, Φ_{BS} with

[1]It is an assumption in this paper that the gateway contains information about the deployment of BS nodes in the secondary system attempting to share resources with the satellite so that the value of the interference temperature constraint is set according to the number of active nodes.

[2]Admittedly, obtaining perfect CSI at the GW is difficult since satellite communication systems experience long round trip delays from the GW to users. However, these studies state that reliable CSI is obtainable by the consideration of fixed satellite services. In addition, recent research efforts are considering precoding paradigms to reduce the dependence of effective precoding on accurate CSI, see [4], [25], [26].

[3]Although, other precoding schemes have been investigated in recent satellite literature, we consider ZF as a simple linear precoder, shown to improve spectral efficiency with a 20–50 % in [3].

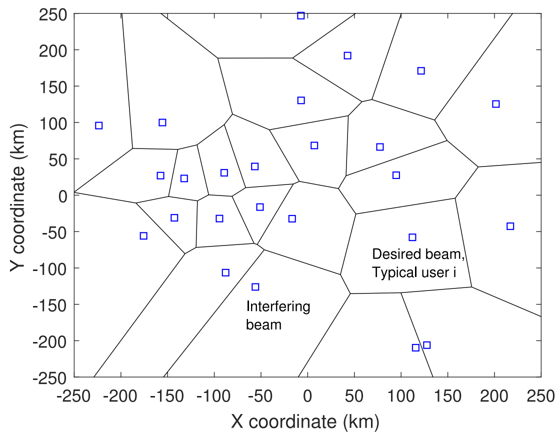

Fig. 2. An illustration of the satellite user network under PPP model showing the location of users in a cluster of K beams. The cell boundaries are shown and form a Voronoi tessellation.

intensity λ_{BS} in $\mathbb{R}^2$. It is assumed that the point processes are independent. For the satellite system, transmissions are simultaneous and use a universal frequency reuse scenario where all users can use the same channel and we consider a typical user receiving information from a multi-beam satellite.

B. Satellite System Model

1) Fading Model: We assume that the forward link contains both the line-of-sight (LOS) component and the scatter component. Hence, consider Ω to be the average receive power of LOS term, b_0 as half of the average power of scattered component, and m as the Nakagami fading coefficient by definition. Leveraging the results from [27], the Shadowed-Rician (SR) fading model can be considered to model both the LOS and scatter components. Therefore the probability density function (PDF) can be written as

$$f_{|h|^2}(x) = \left(\frac{2mb_0}{2mb_0+\Omega}\right)^m \frac{1}{2b_0}\exp\left(-\frac{x}{2b_0}\right) \times {}_1F_1\left(m, 1, \frac{\Omega x}{2b_0(2mb_0+\Omega)}\right) \quad (1)$$

where ${}_1F_1$ is the hypergeometric function and the parameters b_0, m and Ω are connected with the elevation angle θ as illustrated in Fig. 1. We omit the corresponding expressions of parameters b_0, m and Ω as they are characterized in detail in [27]. Although the SR fading model is widely used in literature, the PDF and cumulative density function (CDF) are too complex to work with SINR expressions. Therefore, we approximate the squared SR model with Gamma random variable. Accordingly, the parameters of Gamma random variable are given as [27]

$$\alpha_s = \frac{m(2b_0+\Omega)^2}{4mb_0^2+4mb_0\Omega+\Omega^2}, \quad \beta_s = \frac{4mb_0^2+4mb_0\Omega+\Omega^2}{m(2b_0+\Omega)}. \quad (2)$$

2) Antenna Gain at Satellite User Terminal: It is worth noticing that the average SINRs are highly dependent on both satellite beam pattern and user position. Therefore, the beam gain can be approximated as [3]

$$G_{ii} = \mathcal{L}_{\max} G_{s,i} G_{r,i} \left(\frac{J_1(x)}{2x} + 36\frac{J_3(x)}{x^3}\right)^2 \quad (3)$$

where $\mathcal{L}_{\max}$ is the free space loss [24],[4] $x = 2.07123\sin(\phi_{ii})/\sin(\phi_{3dB})$, J_1 and J_3 are the first-kind Bessel functions of order 1 and 3. $G_{s,i}$ is the satellite transmit antenna gain for the ith beam and $G_{r,i}$ is the satellite user's receive antenna gain. Note that ϕ_{ii} is denoted as the off-axis angle of the ith desired beam, and ϕ_{ij} is the off-axis angle from the ith desired beam to the center of the jth interfering beam. Therefore, G_{ii} can be calculated from (3) with ϕ_{ii}. Similarly, G_{ij} which is the observed antenna gain between the jth interfering beam and the ith user, is also calculated by (3) in terms of ϕ_{ij}.

C. Terrestrial System Model

1) Fading Model: The impact of small scale fading on the transmitted signals of cellular networks is higher than satellite systems. The extensive study of cellular networks in [29] and [30] show that the Nakagami fading model can capture a generalised propagation environment. Hence, we consider Nakagami-m channel model, and the channel power is distributed according to

$$h_i \sim f_\Gamma(x; m_i) \triangleq \frac{m_i^{m_i} x^{m_i-1} e^{-m_i x}}{\Gamma(m_i)}, \quad (4)$$

where $i \triangleq cc, cp$, and $\Gamma(m_i)$ is the gamma function.

2) Directional Beamforming Model: In order to reduce the impact of terrestrial interference on the satellite user terminals, we employ directional beamforming at BSs [20], [31]. Accordingly, multiple antenna arrays are deployed at the transmitters. It is worth noticing that the receiver, i.e., terrestrial user is also equipped with directional antennas. We consider static beamforming though sectorized antennas. Hence, we assume that all the antennas at transmit and receiver pairs are directional antennas with sectorized gain patterns. Let M_{BS} denote the number of transmit antennas at a BS and $\mathrm{M_R}$ denote receive antennas which could either be a satellite or terrestrial user. Denoting the in-sector antenna array gain as G_q^{M} and the out-of-sector antenna array gain as G_q^{m} respectively, these gains are expressed as [32]

$$G_q^{\mathrm{M}} = \frac{\mathrm{M_q}}{1+\delta_q(\mathrm{M_q}-1)},$$
$$G_q^{\mathrm{m}} = \delta_q G_q^{\mathrm{M}}, \quad (5)$$

where $q \in \{\mathrm{BS}, \mathrm{R}\}$, δ_q is a factor that measures the ratio of main lobe to side lobe level. We assume adaptive beamforming at the BSs such that active transmission link is that where maximum gain can be achieved. Thus, for any intended link, q (i.e., the transmission link between a given BS and the terrestrial user), the beamforming gain, $G_q = G_{\mathrm{BS}}^{\mathrm{M}} G_{\mathrm{R}}^{\mathrm{M}}$. The gains

[4] We assume the satellite channel is quasi-stationary which implies that the environmental characteristics including the effect of rain attenuation can be neglected. This is levaraging on the results of experimental data from [28] that shows that the environmental attributes of the channel are assumed to be constant within a small area.

of links other than the intended link will be denoted as G_t. G_t also depends on the in-sector directivity gains (i.e., G^{M}) and out-of-sector (i.e., G^{m}) gains of the antenna beam pattern. Accordingly, the effective antenna gain for an interferer seen by the terrestrial user is given by

$$G_t = \begin{cases} G_{\mathrm{BS}}^{\mathrm{M}} G_{\mathrm{R}}^{\mathrm{M}}, & \mathcal{P}_{MM} = \frac{1}{M_{BS} M_{\mathrm{R}}} \\ G_{\mathrm{BS}}^{\mathrm{M}} G_{\mathrm{R}}^{\mathrm{m}}, & \mathcal{P}_{Mm} = \frac{(M_{\mathrm{R}}-1)}{M_{BS} M_{\mathrm{R}}} \\ G_{\mathrm{BS}}^{\mathrm{m}} G_{\mathrm{R}}^{\mathrm{M}}, & \mathcal{P}_{mM} = \frac{(M_{BS}-1)}{M_{BS} M_{\mathrm{R}}} \\ G_{\mathrm{BS}}^{\mathrm{m}} G_{\mathrm{R}}^{\mathrm{m}}, & \mathcal{P}_{mm} = \frac{(M_{\mathrm{R}}-1)(M_{BS}-1)}{M_{BS} M_{\mathrm{R}}} \end{cases} \tag{6}$$

where $\mathcal{P}_{tk}$, with $t, k \in \{\mathrm{M}, \mathrm{m}\}$ denotes the probability that the antenna gain $G^t G^k$ is seen by the receiver. Here, the effective gain can be considered as a random variable, which can take any of the above-mentioned values.

D. Signal Model

1) Satellite Received Signal: The overall channel gain between the jth beam and ith user of the satellite can be given as

$$h_{pp}^{ij} = h_{pp}^{j} \, G_{ij}(\phi_{ij})^{1/2}, \quad i, j = 1, \ldots, K. \tag{7}$$

Consider P_{si} as the satellite transmit power of ith beam, and x_p^i as the transmitted information symbol from beam i. The received signal at ith beam user can be formulated as

$$y_i = \sqrt{P_{si}}\, G_{ii}\, h_{pp}^{i}\, x_p^{i} + \sum_{j \in \Phi_U, j \neq i} \sqrt{P_{sj}}\, G_{ij}\, h_{pp}^{i}\, x_p^{j} + I_{\mathrm{BS}} + \omega_i \tag{8}$$

where ω_i is the noise power at beam i, P_{sj} is the satellite transmit power of the jth beam and I_{BS} is the terrestrial interference given by

$$I_{\mathrm{BS}} = \sum_{l \in \Phi_{\mathrm{BS}}} \sqrt{P_{\mathrm{ter}}}\, G_t\, h_{cp}^{l}\, x_c^{l}\, r_{l,i}^{-\alpha}, \tag{9}$$

where P_{ter}, x_c^l are the transmit power and information signal from the l^{th} terrestrial BS, $r_{l,i}$ is the distance from l^{th} BS to the i^{th} beam of the satellite user, and α is the path loss exponent.

2) Terrestrial Received Signal: The received signal at the terrestrial user from the l^{th} BS is represented as:

$$y_l = \sqrt{P_{\mathrm{ter}}}\, G_l\, r_l^{-\alpha}\, h_{cc}^{l}\, x_c^{l} + \sum_{m \in \Phi_{\mathrm{BS}}, m \neq l} \sqrt{P_{\mathrm{ter}}}\, G_t\, r_m^{-\alpha} h_{cc}^{m}\, x_c^{m} + I_{\mathrm{SAT}} + \omega_l, \tag{10}$$

where ω_l is additive white Gaussian noise $\omega_l \sim \mathcal{CN}(0, \sigma_l^2)$, I_{SAT} is the interference from the satellite given by

$$I_{\mathrm{SAT}} = \sum_{j \in \Phi_U} \sqrt{P_{sj}}\, G_{ij}\, h_{pc}^{j}\, x_p^{j}, \tag{11}$$

and h_{pc}^j is the interference channel from the j^{th} beam of the satellite to terrestrial user.

To ensure a BS does not cause interference to the satellite system beyond the pre-defined threshold, Υ, its transmit power is further constrained by [14]:

$$P_{\mathrm{ter}} = \min\left(\frac{\Upsilon}{|h_{cp}^{l}|^2}, P_{\mathrm{tot}}\right), \tag{12}$$

where h_{cp} is the interference channel from the BS to the primary user and P_{tot} is the total available power at the l^{th} BS.

E. SINR Model

In this subsection, we consider the SINR obtained at the terrestrial and satellite users respectively.

1) SINR at Terrestrial User: The SINR at the terrestrial user from the l^{th} BS can be formulated from (10) and given as:

$$\zeta_l = \frac{P_{\mathrm{ter}}\, G_l |h_{cc}^{l}|^2 r_l^{-\alpha}}{\sigma_l^2 + I_{\mathrm{BS}} + I_{\mathrm{SAT}}}, \tag{13}$$

where h_{cc}^l is the fading gain of the channel between l^{th} and the terrestrial user, $I_{\mathrm{BS}} = \sum_{m \in \Phi_{\mathrm{BS}}, m \neq l} P_m\, G_t\, |h_{cc}^{m}|^2\, r_m^{-\alpha}$ is the interference from other BSs in Φ_{BS}, $I_{\mathrm{SAT}} = \sum_{j \in \Phi_U} P_{sj}\, G_{ij}\, |h_{pc}^{j}|^2$ represents interferences from each beam of the satellite to terrestrial user, r_l is the distance from the l^{th} BS to the user, σ_l^2 is the noise power.

SINR at Satellite User: The SINR for the intended link i at the i^{th} user can then be formulated as

$$\zeta_i \triangleq \frac{P_{si} G_{ii} |h_{pp}^{i}|^2}{\sigma_i^2 + \sum_{j \in \Phi_u, j \neq i} P_{sj} G_{ij} \left|h_{pp}^{j}\right|^2 + I_{\mathrm{BS}}}, \tag{14}$$

where h_{pp}^i is the channel fading gain at the i^{th} user, σ_i^2 is the noise power, and h_{pp}^j denotes each interference fading gain from other beams to their users, I_{BS} is the interference from the terrestrial system defined in (9).

The second term of the denominator in (14) is zero due to successful ZF precoding.[5] Hence, the SINR for the intended link i at any particular user considering terrestrial interference can be re-written as

$$\hat{\zeta}_i \triangleq \frac{P_{si} G_{ii} |h_{pp}^{i}|^2}{\sigma_i^2 + \sum_{l \in \Phi_{\mathrm{BS}}} P_{\mathrm{ter}}\, G_t\, |h_{cp}^{l}|^2\, r_{l,i}^{-\alpha}}, \tag{15}$$

where $r_{l,i}$ is the distance between l^{th} BS and i^{th} satellite user, and α is the path loss exponent.

F. Performance Metrics

In order to analyse the performance of the system we will use the two fundamental metrics of outage probability and area spectral efficiency.

Outage Probability: This is the probability that outage occurs at either satellite or terrestrial user. Outage occurs when the received SINR falls below an acceptable threshold, T_t that is,

$$\mathcal{P}_{\mathrm{out}}(T_t) = \mathcal{P}(\mathrm{SINR} < T_t). \tag{16}$$

[5]The ZF precoder is designed using the unconstrained optimization method described in [33] such that the powers of all signals are scaled to correspond with the power increase as a result of precoding. As a result, the transmit power is maintained as the same with the case of no precoding.

Area Spectral Efficiency: This metric is presented to measure the utilization of spectrum efficiency of wireless cellular systems. It is defined as the maximum rate per unit bandwidth of a user in a defined coverage area. It can also be described as the average number of successful transmitted bits per unit area and is therefore determined by the outage probability, $\mathcal{P}_{\text{out}}$. Area spectral efficiency, η_{AE} is expressed as [34]

$$\eta_{AE} = \lambda_{\text{BS}}(1 - \mathcal{P}_{\text{out}}) \log_2(1 + T_t), \tag{17}$$

where T_t is the SINR threshold, and λ_{BS} is the BS node density.

III. Transmission Characterisation in Multi-Beam CSTN

Here, we study the performance of the multi-beam CSTN from the perspective of outage probability and area spectral efficiency. In the context of this system model which permits simultaneous transmission of both satellite and terrestrial BSs to their respective users, we consider three practical scenarios. First is the analysis under assumption that all terrestrial BSs obey the constraint by using a limited transmit power defined in (12), (PCI). Second, we investigate the impact of using directional beamforming at the secondary system to limit interference, (DBI). And third, based on the assumption that not all BSs deployed in the secondary system will meet the requirements for transmission, we perform thinning and analyse only the subset of BSs that meet this constraint (BTPI).

Remark 1: The analysis in the paper is done for the outage probability of both satellite and terrestrial systems. However, the area spectral efficiency analysis presented here is done only for the terrestrial system. The main idea behind this consideration is to measure the impact of interference temperature constraint imposed by the satellite on spectral utilization efficiency at the terrestrial system.

A. PCI: Power Constraint to Limit Interference

In this transmission method, we assume that the terrestrial system is equipped with omnidirectional antennas (i.e., no beamforming is used in transmission). Hence, to manage the interference the terrestrial system causes to the satellite system, the transmission power of terrestrial BSs is limited by the interference constraint imposed by the satellite. We also assume that the terrestrial BSs and users utilize single antennas for transmission. Thus, in the sequel we assess the impact of limited transmit power on the outage performance of the both satellite and terrestrial users. The property of joint random variables is used to quantify the limited transmission power and the interferences from the satellite and terrestrial system as the case requires are characterized by the use of moment generating functions and Laplacian functionals respectively.

Outage Probability at the Terrestrial User: At the terrestrial user, outage occurs when the SINR falls below the threshold, T_t. The outage probability from the l^{th} BS is defined as

$$\mathcal{P}_{\text{out}}(T_t) = \mathcal{P}(\zeta_l < T_t). \tag{18}$$

Thus in the following proposition, we present the outage probability of SINR of the terrestrial user for a predefined threshold, T_t.

Proposition 1: The outage probability of the received SINR at the terrestrial user from the l^{th} BS is given at the top of the next page where

$$\mathbb{E}_{I_{\Phi_{\text{BS}}}}\left[\exp\left(\frac{-A\,k\,r_l^{\alpha}\,T_t\,I_{\Phi_{\text{BS}}}}{P_{\text{tot}}}\right)\right] \tag{20}$$

$$= \exp\left(-2\,\pi\,\lambda_{\text{BS}} \int_r^{\infty} \left(1 - \frac{1}{\left(1 + \frac{A\,k\,P_m\,r_l^{\alpha}}{P_{\text{tot}}\,r^{\alpha}}\right)^{m_{cc}}}\right) r\,\mathrm{d}r\right)$$

$$f_{\Gamma}(y) = \frac{m_{cp}^{m_{cp}}\,y^{m_{cp}-1}\,e^{-m_{cp}y}}{\Gamma\left(m_{cp}\right)}, \tag{21}$$

where m_{cp} is the Nakagami fading parameter of the interference channel, $\gamma(.,.)$ is the lower incomplete gamma function, $\Gamma(m_{cp})$ is the gamma function of m_{cp}, and

$$\mathbb{E}_{I_{\text{SAT}}}\left[\exp\left(\frac{-A\,k\,r_l^{\alpha}\,T_t\,I_{\text{SAT}}}{P_{\text{tot}}}\right)\right]$$

$$= \exp\left[-2\pi\,\lambda_U\left(1 - \frac{1}{\left(1 + \frac{A\,k\,T_t\,r_l^{\alpha}\,G_{ij}\,P_{sj}}{\beta_s\,P_{\text{tot}}}\right)}\right)^{\alpha_s}\right] \tag{22}$$

where β_s and α_s are gamma distribution random variable parameters of the satellite.

Proof: Refer Appendix A. ∎

B. Special Case: Approximating BS Interference Using Gamma Variable and Negligible Satellite Interference

The characterisation of BS interference from Proposition 1, equation (20) is provided in terms of Laplacian and probability generating functionals for which closed forms only exist for special choices of its parameters and distribution. Therefore, in order to obtain a more tractable model, we pursue this interference characterisation in terms of their cumulants [35]. Under Rayleigh fading assumption, we approximate the BS interference distribution using the gamma model. In most modern cognitive-satellite networks, the satellite interference to the terrestrial user is not an essential consideration due to it's negligible magnitude compared to the larger values of intra cluster interference power.

Under this consideration of, the distribution of the equivalent aggregate of BS interference path gain is given as

$$\bar{I}_{\text{BS}} = \sum_{m \in \Phi_{\text{BS}}} |h_{cc}^m|^2 r_m^{-\alpha}. \tag{23}$$

By the use of Campbell's theorem, the characteristic function of $\bar{I}_{\text{BS}}$ is computed as [36]

$$\phi_{\bar{I}_{\text{BS}}}(w) = \exp\left(-2\pi\,\lambda_{\text{BS}} \int_{h_{cc}} \int_{\mathbb{R}} \cdot\left[1 - e^{jwxr_m^{-\alpha}}\right] \cdot f_{h_{cc}}(x)\,\mathrm{d}r\mathrm{d}x\right) \tag{24}$$

where $j = \sqrt{-1}$. Using equation (24), we can obtain the corresponding closed forms of the cumulants. Specifically, the n^{th}

$$\mathcal{P}_{\text{out}}(T_t) = \frac{\gamma\left(m_{cp}, \frac{\Upsilon\, m_{cp}}{P_{\text{tot}}}\right)}{\Gamma\left(m_{cp}\right)} \sum_{k=0}^{m_{cc}} \binom{m_{cc}}{k} (-1)^k\, e^{\frac{-A\,k\,r_l^{\alpha}\,T_t \sigma^2}{P_{\text{tot}}}}\, \mathbb{E}_{I_{\Phi_{\text{BS}}}}\left[e^{\frac{-A\,k\,r_l^{\alpha}\,T_t\, I_{\Phi_{\text{BS}}}}{P_{\text{tot}}}} \right] \mathbb{E}_{I_{\text{SAT}}}\left[e^{\frac{-A\,k\,r_l^{\alpha}\,T_t\, I_{\text{SAT}}}{P_{\text{tot}}}} \right]$$
$$+ \sum_{k=0}^{m_{cc}} \binom{m_{cc}}{k} (-1)^k \int_{\frac{\Upsilon}{P_{\text{tot}}}}^{\infty} \mathbb{E}_{I_{\Phi_{\text{BS}}}}\left[e^{\frac{-A\,k\,r_l^{\alpha}\,T_t\, y\, I_{\Phi_{\text{BS}}}}{\Upsilon}} \right] e^{\frac{-A\,k\,r_l^{\alpha}\,T_t\, y \sigma^2}{\Upsilon}}\, \mathbb{E}_{I_{\text{SAT}}}\left[e^{\frac{-A\,k\,r_l^{\alpha}\,T_t\, y\, I_{\text{SAT}}}{\Upsilon}} \right] f_{\Gamma}(y)\, \mathrm{d}y \tag{19}$$

cumulant of $\phi_{\bar{I}_{\text{BS}}}(w)$ can be given by

$$\kappa_{\bar{I}_{\text{BS}}}(n) = \frac{1}{j^n} \frac{\mathrm{d}^n}{\mathrm{d}w^n} \frac{\left(\log \phi_{\bar{I}_{\text{BS}}}(w)\right)}{1}\Big|_{w=0} \tag{25}$$

After integration of equation (24) (refer to [36] for detailed derivations), we obtain

$$\kappa_{\bar{I}_{\text{BS}}}(n) = \frac{2\pi\,\lambda_{\text{BS}}}{n\,\alpha - 2}\, \mathbb{E}_{h_{cc}}\left(h_{cc}^{2/\alpha}\right). \tag{26}$$

To obtain the closed form expressions of $\kappa_{\bar{I}_{\text{BS}}}(n)$ under the Gamma model, we consider the distribution of $\bar{I}_{\text{BS}}$ as

$$f_{\bar{I}_{\text{BS}}}(x; \nu, \theta) = \frac{x^{\nu-1} e^{-\frac{x}{\theta}}}{\theta^{\nu}\Gamma(\nu)}, \tag{27}$$

where the parameters ν and θ are given by

$$\nu = \frac{\kappa_{\bar{I}_{\text{BS}}}(1)}{\kappa_{\bar{I}_{\text{BS}}}(2)} \quad \text{and} \quad \theta = \frac{\kappa_{\bar{I}_{\text{BS}}}(2)}{\kappa_{\bar{I}_{\text{BS}}}(1)}. \tag{28}$$

with the cumulants $\kappa_{\bar{I}_{\text{BS}}}(1)$ and $\kappa_{\bar{I}_{\text{BS}}}(2)$ being characterized using equation (26).

The interested reader is referred to [37], to obtain more insights on the use of gamma variables.

Accordingly, we obtain the closed form expression of outage probability at the terrestrial user in the following proposition.

Proposition 2: The outage probability of the received SINR at the terrestrial user from the l^{th} BS is given as

$$\mathcal{P}_{\text{out}}(T_t) = \gamma\left(1, \frac{\Upsilon}{P_{\text{tot}}}\right) e^{\frac{-A\,r_l^{\alpha}\,T_t \sigma^2}{P_{\text{tot}}}} \left(\frac{A\,r_l^{\alpha}\,T_t\,P_m}{P_{\text{tot}}} + \frac{1}{\theta}\right)^{-\nu}$$
$$\times\ \theta^{-\nu} + e^{\frac{\Upsilon}{P_{\text{tot}}}} - e^{\frac{1+t\sigma^2}{t\theta}} \left(t\frac{\Upsilon}{P_{\text{tot}}} + \frac{1}{\theta}\right)^{-\nu} \theta^{-\nu}$$
$$\times \left(\frac{t\theta}{1+t\theta\frac{\Upsilon}{P_{\text{tot}}}}\right)^{-\nu} \left(1 + t\sigma^2\right)^{-1+\nu}$$
$$\times\ \Gamma\left[1-\nu, \left(\frac{\Upsilon}{P_{\text{tot}}} + \frac{1}{t\theta}\right)\left(1 + t\sigma^2\right)\right] \tag{29}$$

where $t = \frac{A\,r_l^{\alpha}\,T_t\,P_m}{\Upsilon}$.

Proof: See Appendix B. ■

In order to quantify the impact of restricting the transmit power at terrestrial BS on satellite communication, we consider outage probability at the satellite user.

Outage Probability at the Satellite User: Here, outage occurs when the received SINR at the user is less than acceptable threshold, T_s. Thus the outage probability is given in the following proposition.

Proposition 3: The outage probability at the i^{th} beam of the satellite system is given at the top of the next page where $s = \frac{A\,l\,\beta_s\,T_s}{P_{si} G_{ii}}$, $\Gamma(x, y)$, $\gamma(x, y)$, are the upper and lower incomplete gamma functions respectively, and $\Gamma(x)$ is the gamma function.

Proof: See Appendix C. ■

C. DBI: Directional Beamforming to Control Interference

In this scenario, we investigate limiting the interference of secondary system by employing static directional beamforming using sectorized antennas to focus the signals for the terrestrial user. Here, the terrestrial system is assumed to be equipped with M_{BS} antennas at the BSs and M_{R} antennas at the user[6]. We begin with determining the outage probability at the secondary user and then evaluate the impact on the satellite user by measuring its outage probability. This is achieved by using sectorized gain patterns to characterize main lobe and side lobe gains used in transmission. The interference from BSs other than the transmitting BS is quantified with Laplace functionals.

The following proposition gives the effect of applying directional beamforming on the terrestrial user's outage performance.

Proposition 4: The outage probability at the terrestrial user from the l^{th} BS employing directional beamforming for transmission is given as

$$\mathcal{P}_{\text{out}}(T_t) = \sum_{k=0}^{m_{cc}} \binom{m_{cc}}{k} (-1)^k$$
$$\times\ \exp\left(\frac{-A\,k\,r_l^{\alpha}\,T_t\sigma^2}{P_{\text{ter}}\,G_l}\right) \mathbb{E}_{I_{\text{SAT}}}\left[e^{\frac{-A\,k\,r_l^{\alpha}\,T_t I_{\text{SAT}}}{P_{\text{ter}}\,G_l}} \right] \prod_{t,k\in\{\text{M},\text{m}\}}$$
$$\times\ \exp\left[-2\pi\,\mathcal{P}_{tk}\lambda_{\text{BS}} \int_{r}^{\infty} \left(1 - \frac{1}{\left(1 + \frac{A\,k\,r_l^{\alpha}\,T_t\,P_m G_t^{tk}}{P_{\text{ter}}\,G_l m_{cc} r_m^{\alpha}}\right)^{m_{cc}}}\right) r\,\mathrm{d}r \right]. \tag{31}$$

Proof: From the proof of Proposition 1, we have

$$\mathcal{P}_{\text{out}}(T_t) = \sum_{k=0}^{m_{cc}} \binom{m_{cc}}{k} (-1)^k e^{\frac{-A\,k\,r_l^{\alpha}\,T_t\sigma^2}{P_{\text{ter}}\,G_l}}$$
$$\times\ \mathbb{E}_{I_{\text{BS}}}\left[e^{\frac{-A\,k\,r_l^{\alpha}\,T_t\,I_{\Phi_{\text{BS}}}}{P_{\text{tot}}\,G_t}} \right] \mathbb{E}_{I_{\text{SAT}}}\left[e^{\frac{-A\,k\,r_l^{\alpha}\,T_t\,I_{\text{SAT}}}{P_{\text{ter}}\,G_l}} \right]. \tag{32}$$

[6]This assumption is justified since when employing directional beamforming, the multiple transmit and receive antennas form a transmit beam and a receive beam which is equivalent to communication with a single directional transmit antenna and a single directional receive antenna [38], [39].

$$\mathcal{P}_{\text{out}}(T_s) \approx \sum_{l=0}^{\alpha_s} \binom{\alpha_s}{l} (-1)^l \exp\left(-s\sigma_i^2\right) \exp\Bigg[2\pi\lambda_{\text{BS}}\Bigg(\int_r^{\infty} \frac{m_{cp}\Gamma\left(m_{cp}, \frac{\Upsilon m_{cp}}{P_{\text{tot}}}\right) - \Gamma(m_{cp}+1)}{m_{cp}\Gamma(m_{cp})} + \frac{m_{cp}^{m_{cp}-1}}{\Gamma(m_{cp})}\left(m_{cp} + P_{\text{tot}} r^{-\alpha} s\right)^{-m_{cp}} \times \left(\Gamma\left(m_{cp}+1\right) - m_{cp}\Gamma\left(m_{cp}, \frac{\Upsilon\left(m_{cp}+P_{\text{tot}}r^{-\alpha}s\right)}{P_{\text{tot}}}\right)\right) + \left(1 - e^{-s\Upsilon r^{-\alpha}}\right)\left(\frac{\gamma\left(m_{cp}, \frac{\Upsilon m_{cp}}{P_{\text{tot}}}\right) - \Gamma\left(m_{cp}\right)}{\Gamma\left(m_{cp}\right)}\right)\Bigg) r\mathrm{d}r\Bigg] \tag{30}$$

However, the terrestrial interference due to other BSs needs to be characterized before proceeding. Given that the interference from BSs could be either from main lobe or side lobe as defined in (6), we utilize the notion of marked stochastic geometry to characterize the interference as [40]

$$I_{\Phi_{\text{BS}}} = I_{\Phi_{\text{BS}}}^{MM} + I_{\Phi_{\text{BS}}}^{Mm} + I_{\Phi_{\text{BS}}}^{mM} + I_{\Phi_{\text{BS}}}^{mm}. \tag{33}$$

By definition of the Laplace transform, we have

$$\mathcal{L}\{I_{\Phi_{\text{BS}}}\} = \mathcal{L}\{I_{\Phi_{\text{BS}}}^{MM}\}\mathcal{L}\{I_{\Phi_{\text{BS}}}^{Mm}\}\mathcal{L}\{I_{\Phi_{\text{BS}}}^{mM}\}\mathcal{L}\{I_{\Phi_{\text{BS}}}^{mm}\}. \tag{34}$$

Starting with the characterisation of $\mathcal{L}\{I_{\Phi_{\text{BS}}}^{MM}\}(s)$, we obtain

$$\begin{aligned}
\mathcal{L}\{I_{\Phi_{\text{BS}}}^{MM}\}(s) &= \mathbb{E}\left[\exp\left(-s I_{\Phi_{\text{BS}}}^{MM}\right)\right], \\
&= \mathbb{E}_{\Phi_{\text{BS}}, h_{cc}^m, G_t}\left[\exp\left(-s P_m G_t^{MM} |h_{cc}^m|^2 r_m^{-\alpha}\right)\right], \\
&\overset{(a)}{=} \mathbb{E}_{\Phi_{\text{BS}}, G_t}\left\{\prod_{m\in\Phi_{\text{BS}}}\left(\frac{1}{1+\frac{s P_m G_t^{MM} r_m^{-\alpha}}{m_{cc}}}\right)^{m_{cc}}\right\}, \\
&\overset{(b)}{=} \mathbb{E}_{G_t}\left\{\exp\left[-2\pi \mathcal{P}_{MM}\lambda_{\text{BS}} r\left(1 - \frac{1}{\left(1+\frac{s P_m G_t^{MM}}{m_{cc} r_m^{\alpha}}\right)^{m_{cc}}}\right)\mathrm{d}r\right]\right\},
\end{aligned} \tag{35}$$

where $\mathcal{P}_{MM}$ is the probability that $G_t^{MM} = G^M G^M$, $s = \frac{A\,k\,r_l^{\alpha}\,T_t}{P_{\text{ter}}\,G_l}$, (a) follows from the use of the moment generating function of Gamma random variable with Nakagami fading parameter m_{cc}, and (b) follows due to the use of probability generating functionals of PPPs. Following similar steps, $\mathcal{L}\{I_{\Phi_{\text{BS}}}^{Mm}\}$, $\mathcal{L}\{I_{\Phi_{\text{BS}}}^{mM}\}$, $\mathcal{L}\{I_{\Phi_{\text{BS}}}^{mm}\}$ can be computed and finally, using equation (34), the Laplace transform of $I_{\Phi_{\text{BS}}}$ is given as

$$\begin{aligned}
\mathcal{L}\{I_{\Phi_{\text{BS}}}\}(s) &= \mathbb{E}[\exp(-s I_{\Phi_{\text{BS}}})], \\
&= \prod_{t,k\in\{\text{M},\text{m}\}} \exp\left[-2\pi \mathcal{P}_{tk}\lambda_{\text{BS}} r\left(1 - \frac{1}{\left(1+\frac{s P_m G_t^{tk}}{m_{cc} r_m^{\alpha}}\right)^{m_{cc}}}\right)\mathrm{d}r\right]
\end{aligned} \tag{36}$$

where r_m is the distance between the m^{th} BS and the terrestrial user. The characterisation of $\mathcal{L}\{I_{\text{SAT}}\}(s)$ has been outlined in Appendix A and is expressed as

$$\mathcal{L}\{I_{\text{SAT}}\}(s) = \exp\left[-2\pi\lambda_U\left(1 - \frac{1}{\left(1+\frac{s\,G_{ij}\,P_{sj}}{\beta_s}\right)^{\alpha_s}}\right)\right], \tag{37}$$

where $s = \frac{A\,k\,r_l^{\alpha}\,T_t}{P_{\text{ter}}\,G_l}$, α_s and β_s are the gamma distribution parameters of the satellite given in (2).

This proof is concluded by substituting (36) and (37) into (32). ■

Outage Probability at Satellite User: In the following lemma we measure the impact of employing directional beamforming at the terrestrial BS in terms of outage probability at the satellite user.

Lemma 1: The outage probability of at the i^{th} user of the satellite considering directional beamforming at the terrestrial system is given as

$$\begin{aligned}
\mathcal{P}_{\text{out}}(T_s) \approx &\sum_{l=0}^{\alpha_s}\binom{\alpha_s}{l}(-1)^l \exp\left(\frac{-A\,l\,\beta_s\,T_s\sigma^2}{P_{si}G_{ii}}\right)\prod_{t,k\in\{\text{M},\text{m}\}} \\
&\times \exp\left[-2\pi\mathcal{P}_{tk}\lambda_{\text{BS}}\int_r^{\infty}\left(1 - \frac{1}{\left(1+\frac{A\,l\,\beta_s\,T_s\,P_{\text{ter}}G_t^{tk}}{P_{si}G_{ii}m_{cp}r_{l,i}^{\alpha}}\right)^{m_{cp}}}\right) r\,\mathrm{d}r\right],
\end{aligned} \tag{38}$$

where $r_{l,i}$ is the distance from the l^{th} BS to the i^{th} satellite user.

Proof: The proof follows from Proposition 4. ■

Remark 2: It is important to note that with single transmit and receive antennas, directional beamforming cannot be used to manage the interference. Hence, limiting the transmit power of the terrestrial system as in PCI is the method employed. In other words, when $\text{M}_{\text{BS}} = \text{M}_{\text{R}} = 1$, then DBI reduces to PCI.

D. BTPI: BS Thinning Process to Restrict Interference

In this subsection, we characterize BSs which do not satisfy the interference constraint imposed by primary system. As some of the BSs may not provide sufficient coverage for the terrestrial user, and these BSs may override the interference temperature constraint set by satellite system and may cause harmful interference to primary users, leading to a deterioration of the system's performance. In such conditions, one can make use of a thinning operation on the original PPP of BSs, leading to the well-known Matern Hard-core point process (MHCPP) that has been used to appropriately model networks with guard zones [41].

Additionally, for power constrained terrestrial systems, the characterisation of hardcore models of point processes needs to take into consideration fading and interference constraint. In this regard, thinning with respect to fading is considered. We leverage the results from [41] and [42] and incorporate thinning in the design aspects of our system model. The characterization of HCPP models via the Laplace functional and probability generating functionals is quite difficult to analyse

$$\mathcal{P}_{\Xi} = \Big[\tfrac{\pi \operatorname{Csc}\left[(m_{ij}-m_{cp})\pi\right]}{\Gamma\left[m_{ij}\right]\Gamma\left[m_{cp}\right]}\Big(-m_{ij}^{m_{ij}}\left(\tfrac{m_{cp}\,\Upsilon\, r_c^{\alpha}}{P_t}\right)^{m_{ij}}\Gamma\left[m_{ij}\right]{}_P F_{\Upsilon}\Big[\left\{m_{ij}\right\},\left\{1+m_{ij},1+m_{ij}-m_{cp}\right\},m_{ij}\,m_{cp}\tfrac{\Upsilon\, r_c^{\alpha}}{P_t}\Big] + m_{ij}^{m_{cp}}\left(\tfrac{m_{cp}\,\Upsilon\, r_c^{\alpha}}{P_t}\right)^{m_{cp}}\Gamma\left[m_{cp}\right]{}_P F_{\Upsilon}\Big[\left\{m_{cp}\right\},\left\{1+m_{cp},1-m_{ij}+m_{cp}\right\},m_{ij}\,m_{cp}\tfrac{\Upsilon\, r_c^{\alpha}}{P_t}\Big]\Big)\Big] \tag{42}$$

and has not been properly done yet. However, the nodes further away from a hard core distance, d, can still be modelled as a PPP as shown in [42]. Thus, we take into account such an approximation for analytical tractability, and consider that the distribution of BSs follows a PPP while their density is approximated by that of the density of a modified hard-core PPP, $\bar{\lambda}_{\text{BS}}$.

Let Φ_{BS} be the primary point process and $\bar{\Phi}_{\text{BS}}$ be the generalised MHCPP. In order to generalise the traditional MHCPP with respect to transmit power with interference constraint, the hard-core distance d is replaced with the received power.

Remark 3: A BS node is retained in $\bar{\Phi}_{\text{BS}}$ if, and only if, it has the lowest mark in its neighborhood set of BSs, $N(x_i)$ determined by dynamically changing the random-shaped region defined by instantaneous path gains, which can be looked upon as the communication range.

Lemma 2: Let the number of BSs in communication range be N, the retaining probability of a BS node is $\mathcal{P}_{\text{BS}} = \frac{1-e^{-N\mathcal{P}_{\Xi}}}{N\mathcal{P}_{\Xi}}$. Then the intensity of active number of BSs is given by $\bar{\lambda}_{\text{BS}} = \lambda_{\text{BS}}\mathcal{P}_{\text{BS}}$ [41, Th. 4.1].

Now, in order to find $\mathcal{P}_{\text{BS}}$, we have to compute the neighbourhood success probability $\mathcal{P}_{\Xi}$. Let x_i represent the location of a BS in Φ_{BS}, i.e., $i \in \Phi_{\text{BS}}$. The neighbourhood set of any BS located at x_i is determined by bounding an observation region, $\mathcal{B}_{x_i}$ by $\mathcal{B}_{x_i}(r_d)$, where r_d is a sufficiently large distance, such that the probability that any BS located beyond r_d becomes neighbour of the BS at x_i is a very small number, ϱ. This probability is expressed as

$$\mathcal{P}\left\{\frac{P_t\,|h_{ij}|^2}{||x_i-x_j||^{\alpha}} \leq \tfrac{\Upsilon}{|h_{cp}|^2}\,|\,||x_i-x_j|| > r_d\right\} \leq \varrho, \tag{39}$$

where P_t is the transmit power of any BS, x_i and x_j represent the locations of any two BSs in Φ_{BS}, and $||x_i - x_j||$ is the distance between two neighbouring BSs.

Then the neighbourhood success probability within the bounded region can be defined as

$$\mathcal{P}_{\Xi} = \mathcal{P}\left\{\Psi_{x_i,x_j} \leq \tfrac{\Upsilon}{|h_{cp}|^2}|x_j \in \mathcal{B}_{x_i}(r_d)\right\}, \tag{40}$$

where $\Psi_{x_i,x_j} = \dfrac{P_t\,|h_{ij}|^2}{r_c^{\alpha}}$, and $r_c = ||x_i - x_j||$ is the distance between any two BSs in comparison.

Following from ratio and product distribution [40], (40) can be written as

$$\mathcal{P}_{\Xi} = \int_0^{\infty}\int_0^{\frac{\Upsilon\, r_c^{\alpha}}{P_t}} f_{|h_{ij}|^2}(x) f_{|h_{cp}|^2}\left(\tfrac{y}{x}\right)\tfrac{1}{x}\mathrm{d}y\,\mathrm{d}x,$$

$$= \int_0^{\infty} f_{|h_{ij}|^2}(x) F_{|h_{cp}|^2}\left(\frac{\Upsilon\, r_c^{\alpha}}{P_t\, x}\right)\mathrm{d}x. \tag{41}$$

Using (41), we can derive the generalised MHCPP process of the BSs and their active nodes which satisfy the interference constraint. Therefore, the closed-form expression of the above integral is given at the top of this page, where ${}_P F_{\Upsilon}$ is the hypergeometric regularised function, m_{ij} is the Nakagami fading parameter from the distribution of h_{ij} and Csc is cosecant function.

From the above analysis, the outage probability at the terrestrial and satellite users can be computed with the updated density, $\bar{\lambda}_{\text{BS}}$, by following steps similar to proposition 3 and lemma 1 respectively.[7]

IV. Numerical Results

As previously mentioned, we have analysed three different methods of limiting interference caused by terrestrial communication to the satellite network. In this section, we provide numerical results to validate our system model and present comparison of these three interference limiting schemes. We also verify the accuracy of theoretical results presented in the previous section showcasing the performance metrics of outage probability and area spectral efficiency. The parameters considered for simulation in this paper are inspired from related studies on CSTNs, satellite and cellular communication [16], [27], [31] and the correctness of the analytical results is verified through Monte Carlo simulations. For the primary satellite network, we consider a K-beam network with an orbit radius of 35786 km where the intensity of satellite users is expressed as $\lambda_U = \frac{K}{\pi R^2}$ where K is any integer that indicates the average number of users/beams being served by the satellite. A few of the parameters with their corresponding values are presented in Table I. All other parameters will be explicitly mentioned wherever used.

Figures 3 to 5 illustrate the impact of limiting terrestrial BS transmit power using the imposed interference temperature constraint (PCI). In Fig. 3, we compare the outage probability performance with different values of satellite imposed interference temperature constraint at the terrestrial user. This result is a validation of proposition 1. It can be observed that the simulation results obtained from the numerical evaluation of equation (19) are consistent with the analytical derivations, as shown by the matching of these results. As can be seen, with increasing values of interference temperature constraint, Υ, the outage probability performance is considerably lower. This result is expected as increasing the interference temperature constraint implies that the terrestrial BS can transmit

[7]It is important to note that although the expressions for outage probability are not presented in closed form, they are not computationally complex and can easily and efficiently be calculated with the use of many computer software programmes including MATLAB and MATHEMATICA.

TABLE I
SIMULATION PARAMETERS

Notation	Parameter	Values
d_0	Orbit	35786 Km
r_d	Beam radius	50 Km
$G_{s,i}$	Satellite antenna gain	30 dBi
$G_{r,i}$	Satellite terminal gain	15 dBi
$3dB$	Angle	0.4^o
ϕ_{ii}	Off-axis angle of desired user	0.6^o
ϕ_{ij}	Off-axis angle of interfering user	0.8^o
λ_{S}	Density of users	1e-10
λ_{BS}	Density of BSs	5e-06
G^M	BS antenna gain of main lobe	15 dB
α	Path loss exponent	2.1
P_{ter}	Node transmit power	20 dB
m_{cc}, m_{cp}	Nakagami parameter	1
N_0	Noise power	-174 dB

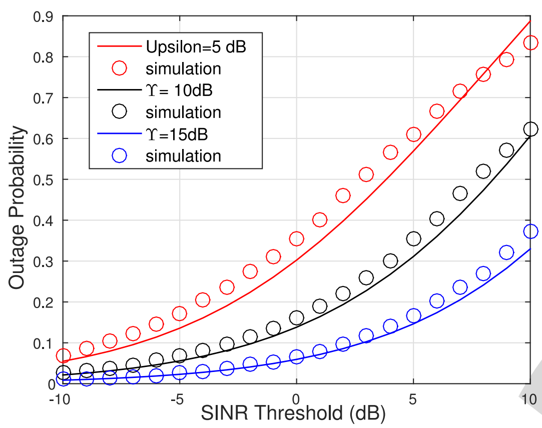

Fig. 3. Outage probability as a function of SINR threshold of the secondary network under different satellite interference temperature constraints, Υ and $P_{\mathrm{tot}} = 20$ dB.

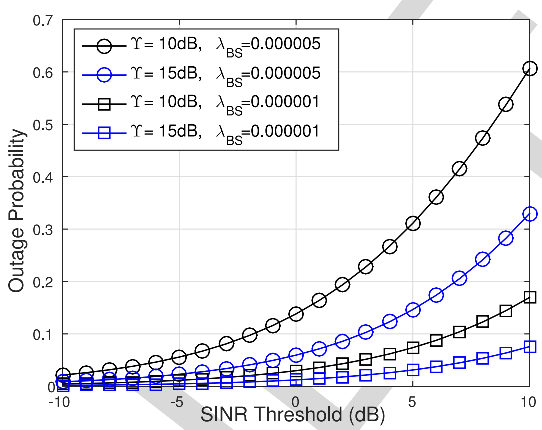

Fig. 4. Outage probability as a function of SINR threshold of the secondary network with varying BS node density under different satellite interference temperature constraints, Υ.

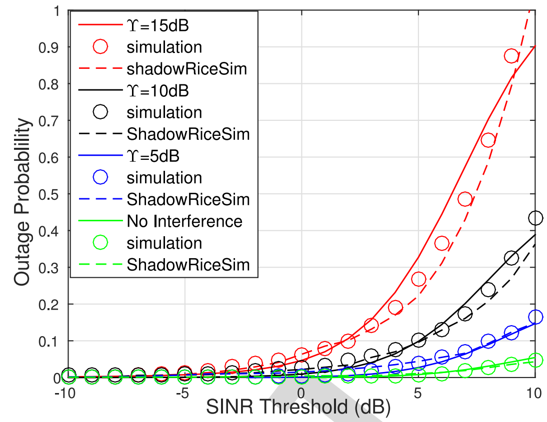

Fig. 5. Outage probability at the satellite user as a function of SINR threshold for varying interference temperature constraints, Υ, $P_{\mathrm{tot}} = 20$ dB.

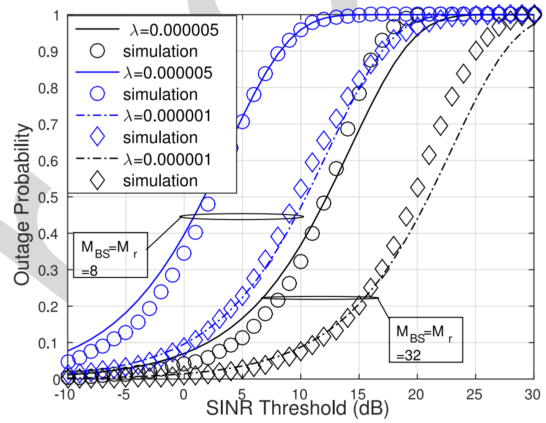

Fig. 6. Outage probability at the terrestrial user as a function of SINR threshold for varying BS node density with varying antenna gain.

with more power, which in turn leads to more successful communication with the terrestrial user.

After establishing that increased interference temperature constraint has a positive impact on terrestrial communication, we now consider the effect of node density, λ_{BS}, on the outage. Hence, in Fig. 4, we present a plot of outage probability against SINR threshold at the terrestrial user for varying values of λ_{BS} and Υ. As can be observed, reducing the BS density leads to a decrease in outage probability. This outcome can be explained by the fact that a higher density of BSs (implying more deployed BSs) indicate that there are many more BSs to interfere with the intended transmission to the terrestrial user. Also, confirming the results from Fig. 3, the outage probability is lower for $\Upsilon = 15$ dB in both cases of λ_{BS} when compared with values for $\Upsilon = 10$ dB.

In Fig. 5, we analyse the outage probability at the satellite user with respect to restricting the transmit power of the terrestrial base stations. To provide more insight on the impact of constraint in the CSTN, we compare these results to the case of no interference (non-transmitting terrestrial BSs). It can be seen from the figure that outage probability is appreciably lower with decreasing values of interference temperature constraint. This result is in contrast to the observations of varying constraint at the terrestrial user in Fig. 4, and this outcome implies that lowering the values of interference temperature constraint produces more rigidity in restraining the transmission power of terrestrial BSs, which then results in noticeably lower interference to the satellite user and lesser probablity of outage. In addition, we provide simulation results of the satellite channel using the SR fading model; as can be observed from the figure, the simulations are closely matched with the simulations using the Gamma random variable approximation

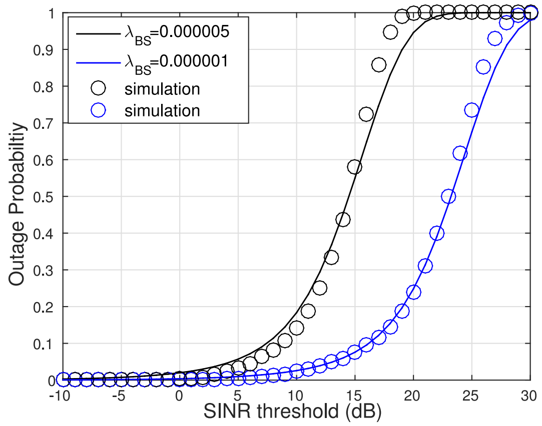

Fig. 7. Outage probability at the satellite user as a function of SINR threshold for varying BS node density when terrestrial BS is employing beamforming with M_{BS}=32, $M_r = 16$, $\alpha = 2.5$.

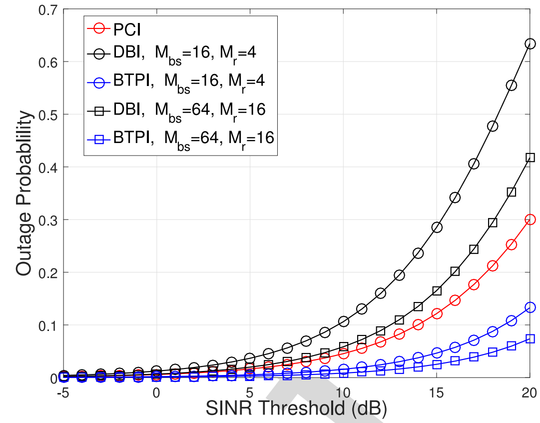

Fig. 8. Comparison of outage probability at the terrestrial user using three methods for $\Upsilon = 0$ dB, $\lambda_{BS} = 0.000009$.

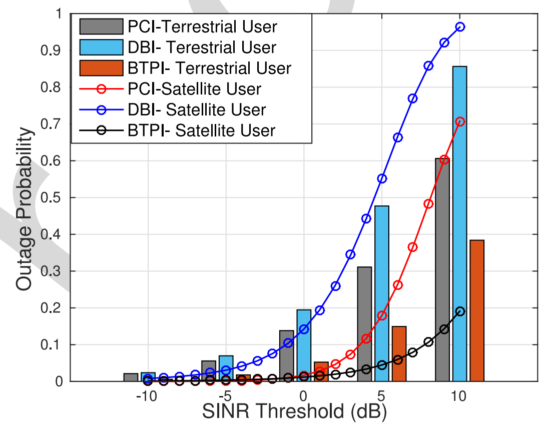

Fig. 9. Comparison of outage probability at both the satellite user and terrestrial user using three methods for $\Upsilon = 10$ dB, $M_{BS} = M_r = 16$.

for the channel. This result is an affirmation of the channel approximation we used in our analysis.

Next, we consider the use of directional beamforming for transmission in the terrestrial system. Fig. 6 presents a comparison of outage probability with different BS densities and antenna gains at the terrestrial user. This result verifies proposition 4 as shown by the minimal performance gap between simulation and analytical results. It can be observed that when the antenna gain is increased, there is a reduction in outage probability. For example, when $\lambda = 0.000001$, for a specific threshold of 10 dB, the outage probability is 0.5 when $M_{BS} = M_r = 8$ whereas when utilizing 32 antennas at both BS and user, the outage probability reduces to 0.1. This result indicates that directional beamforming has a direct effect on the SINR threshold as an increase in the directional beamforming gain results in a reduction in the target SINR threshold required for good coverage. It is also evident from the figure that a higher network density yields more outage for a target SINR value.

The impact at the satellite user of utilizing directional beamforming for terrestrial transmission and interference mitigation is shown in Fig. 7. It can be identified from the figure that as BS nodal density increases, the probability of outage at the satellite user also increases similar to the effect at the terrestrial user. Also worthy of note, deploying more BSs in the terrestrial network increases the aggregate interference caused to the satellite user.

Next, we present the analysis of thinning out all BSs that do not satisfy the interference temperature constraint imposed by the satellite, as discussed in Section III. After thinning, $\bar{\lambda}_{BS}$ is computed using lemma 2 so that, $\bar{\lambda}_{BS} = \lambda_{BS}\mathcal{P}_{BS}$. Accordingly, in Figures 8 and 9, we present a comparison of outage probability by using all three methods of PCI, DBI and BTPI.

Fig. 8 plots the outage probability as a function of SINR threshold at the terrestrial user. It is evident from the figure that for a fixed interference temperature constraint $\Upsilon = 0$ dB, BTPI has the best performance giving the least outage probability for a given target SINR. What is striking about the performance of DBI is its dependence on the antenna array size. Increasing the number of transmit and receive antennas reasonably reduces the outage probability, but this comes at a cost. We note that the gains of employing directional beamforming are optimal when utilizing massive multiple input-multiple output (MIMO) systems, or employing millimeter wave links at the terrestrial system because each of these methods allow for a large array of antennas. This can be investigated in our future work.

Fig. 9 considers the impact of using all three schemes at both the satellite user and terrestrial user. It is apparent that for a target SINR, BTPI is the best method in both cases to reduce the impact of interference on the satellite system in a multi-beam CSTN as its performance results in fewer outages. This result can be explained by the fact that thinning is a strict implementation of the interference temperature constraint imposed by the satellite. DBI gives the worst performance causing the most interference to satellite transmission and increasing the probability of outage occurrences. We note that using PCI, which restricts transmit power at the terrestrial BS, results in moderate interference to the satellite user, much lower than that produced by directional beamforming. Therefore, for a conventional multi-beam CSTN, where thinning is not feasible, PCI is a more viable scheme than DBI but at cost of moderate interference to satellite user.

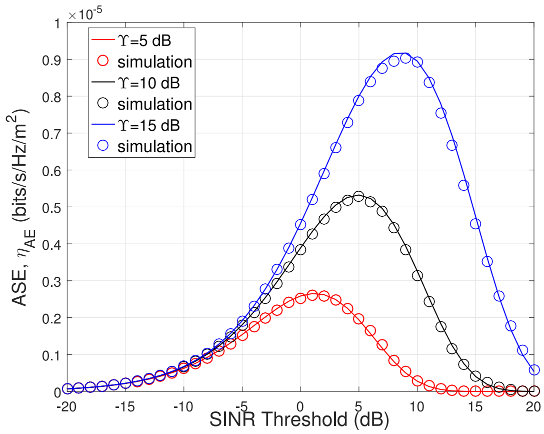

Fig. 10. Area spectral efficiency as a function of SINR threshold for varying interference temperature constraints, Υ.

Finally, in Fig. 10, we illustrate the area spectral efficiency at the terrestrial user with respect to SINR threshold under different values of Υ. It can be seen from the figure that for higher values of interference temperature constraint, the area spectral efficiency increases, which implies that the terrestrial BS can transmit with more power. This outcome is the evidence for reduced outage probability observed at the terrestrial user for increasing values of Υ. It is worthy of mention that there is an optimal value of area spectral efficiency as indicated by the shape of the curves in Fig. 10 with the implication that increasing the SINR threshold has a diminishing returns effect. Further, when the optimal SINR threshold is determined, this can be used to determine the optimal BS density which maximises the area spectral efficiency of the terrestrial system whilst taking into account the constraint imposed by the satellite system. Determination of these optimal points can be explored in future works.

V. Conclusion

The impact of interference in a multi-beam CSTN was investigated. From our analysis, it is clear that successful transmission at both satellite and terrestrial systems depends on network conditions such as BS node density, antenna gain, and interference temperature constraint imposed by the satellite. Accordingly, performance metrics of outage probability and area spectral efficiency were analysed. With simulation results we show the effect of varying the network parameters such as BS node density and the value of interference temperature constraint on the network. After comparing three secondary system transmission schemes (PCI, DBI and BPTI) aimed at keeping interference to the satellite system within the predefined limits, we observed that for a target SINR, BTPI (which strictly adheres to the satellite's requirements) gives the best performance. We also showed that for conventional terrestrial mobile networks, DBI performed the worst. However, the performance when utilizing directional beamforming can be improved at the cost of increasing the antenna gain. In practical scenarios, this would mean employing massive MIMO transceivers or millimeter wave links at the terrestrial system. In addition, when BS thinning is not feasible, restricting the transmit power at the terrestrial BS by lowering the value of interference temperature constraint is the viable method to obtain reduced outage probability of the satellite communication.

Appendix A
Proof of Proposition 1

The terrestrial user experiences outage when its SINR[8] falls below the predefined threshold T_t such that:

$$\begin{aligned}\mathcal{P}_{\text{out}}(T_t) &= \mathcal{P}(\text{SINR} < T_t),\\ &= \mathcal{P}\left(\frac{P_{\text{ter}}\ |h^l_{cc}|^2 r_l^{-\alpha}}{\sigma^2 + I_{\text{BS}} + I_{\text{SAT}}} < T_t\right). \end{aligned} \tag{43}$$

Substituting P_{ter} in (43) with the interference temperature constraint defined in (12) as

$$P_{\text{ter}} = \min\left(\frac{\Upsilon}{|h^l_{cp}|^2}, P_{\text{tot}}\right), \tag{44}$$

and using the property of joint distribution of random variables X and Y from [43], we have:

$$\mathcal{P}(\min(X,Y) < t) = \mathcal{P}(X < t, Y < t),$$

and

$$\min(X,Y) = \begin{cases} X & \text{if } Y > X,\\ Y & \text{if } Y \le X. \end{cases} \tag{45}$$

Therefore, (43) becomes

$$\begin{aligned}\mathcal{P}_{\text{out}}(T_t) &= \mathcal{P}\left(\frac{P_{\text{tot}}\ |h^l_{cc}|^2 r_l^{-\alpha}}{\sigma^2 + I_{\text{BS}} + I_{\text{SAT}}} < T_t, P_{\text{tot}} \le \frac{\Upsilon}{|h^l_{cp}|^2}\right)\\ &\quad + \mathcal{P}\left(\frac{\frac{\Upsilon}{|h^l_{cp}|^2}\ |h^l_{cc}|^2 r_l^{-\alpha}}{\sigma^2 + I_{\text{BS}} + I_{\text{SAT}}} < T_t, P_{\text{tot}} > \frac{\Upsilon}{|h^l_{cp}|^2}\right). \end{aligned} \tag{46}$$

Let $\Gamma = |h^l_{cp}|^2$. The outage probability conditioned on Γ is defined as:

$$\begin{aligned}\mathcal{P}_{\text{out}|\Gamma}(T_t) &= \underbrace{\int_0^{\frac{\Upsilon}{P_{\text{tot}}}} \mathcal{P}\left[\frac{P_{\text{tot}}\ |h^l_{cc}|^2 r_l^{-\alpha}}{\sigma^2 + I_{\text{BS}} + I_{\text{SAT}}} < T_t\right] f_\Gamma(y)\,\text{d}y}_{I}\\ &\quad + \underbrace{\int_{\frac{\Upsilon}{P_{\text{tot}}}}^{\infty} \mathcal{P}\left[\frac{\frac{\Upsilon}{\Gamma}\ |h^l_{cc}|^2 r_l^{-\alpha}}{\sigma^2 + I_{\text{BS}} + I_{\text{SAT}}} < T_t\right] f_\Gamma(y)\,\text{d}y.}_{II} \end{aligned} \tag{47}$$

[8] In this scenario, since we limit the interference using interference temperature constraint, the beamforming gain, $G_l = 1$ and is omitted for subsequent analysis.

Given that fading of the channel of the l^{th} BS , h_{cc}^{l} follows the Nakagami fading model described in Section II-C1, we employ the upper bound approximation of gamma distribution with parameter m_{cc} such that: $\mathcal{P}[\,|h_{cc}^{l}|^2 < \gamma < (1-e^{-A\gamma})^{m_{cc}}]$ with $A = m_{cc}(m_{cc}!)^{\frac{-1}{m_{cc}}}$, therefore, starting with I, the conditional outage probability is expressed as:

$$\mathcal{P}_{\text{out}|\Gamma}^{I}(T_t) = \int_{0}^{\frac{\Upsilon}{P_{\text{tot}}}} \mathcal{P}\left[\frac{P_{\text{tot}}\ |h_{cc}^{l}|^2 r_l^{-\alpha}}{\sigma^2 + I_{\text{BS}} + I_{\text{SAT}}} < T_t\right] f_\Gamma(y)\,\text{dy}, \tag{48}$$

where $f_\Gamma(y)$ is the density of fading of interference channel given by

$$f_\Gamma(y; m_{cp}) = \frac{m_{cp}^{m_{cp}}\, y^{m_{cp}-1} e^{-m_{cp}y}}{\Gamma(m_{cp})}, \tag{49}$$

where m_{cp} is the Nakagami fading parameter, and $\Gamma(m_{cp})$ is the Gamma function,

$$\begin{aligned}
&\mathcal{P}\left[\frac{P_{\text{tot}}\ |h_{cc}^{l}|^2 r_l^{-\alpha}}{\sigma^2 + I_{\text{BS}} + I_{\text{SAT}}} < T_t\right] \\
&= \mathbb{E}_{I_{\text{BS}},I_{\text{SAT}}}\left[\mathcal{P}\left[|h_{cc}^{l}|^2 < \frac{T_t r_l^{\alpha}}{P_{\text{tot}}}\left(\sigma^2 + I_{\text{BS}} + I_{\text{SAT}}\right)\right]\right], \\
&\overset{(a)}{=} \mathbb{E}_{I_{\text{BS}},I_{\text{SAT}}}\left[\left(1 - e^{-A\frac{r_l^{\alpha} T_t}{P_{\text{tot}}}(\sigma^2 + I_{\text{BS}} + I_{\text{SAT}})}\right)^{m_{cc}}\right], \\
&\overset{(b)}{=} \sum_{k=0}^{m_{cc}} \binom{m_{cc}}{k}(-1)^k e^{\frac{-A k r_l^{\alpha} T_t \sigma^2}{P_{\text{tot}}}}\, \mathbb{E}_{I_{\text{BS}}}\left[e^{-\frac{-A k r_l^{\alpha} T_t I_{\text{BS}}}{P_{\text{tot}}}}\right] \\
&\quad \times \mathbb{E}_{I_{\text{SAT}}}\left[e^{-\frac{-A k r_l^{\alpha} T_t I_{\text{SAT}}}{P_{\text{tot}}}}\right], \\
&\overset{(c)}{=} \sum_{k=0}^{m_{cc}} \binom{m_{cc}}{k}(-1)^k e^{\frac{-A k r_l^{\alpha} T_t \sigma^2}{P_{\text{tot}}}} \prod_{m\in\Phi_{\text{BS}}} \mathbb{E}_{I_{\text{BS}}}\left[e^{-\frac{-A k r_l^{\alpha} T_t I_{\text{BS}}}{P_{\text{tot}}}}\right] \\
&\quad \times \prod_{j\in\Phi_U} \mathbb{E}_{I_{\text{SAT}}}\left[e^{-\frac{-A k r_l^{\alpha} T_t I_{\text{SAT}}}{P_{\text{tot}}}}\right],
\end{aligned} \tag{50}$$

where (a) follows from the tight gamma approximation previously defined, (b) follows from applying binomial expansion, and (c) follows from the product of both satellite and terrestrial links such that $I_{\text{BS}} = \sum_{m\in\Phi_{\text{BS}}, m\neq l} P_m |h_{cc}^{m}|^2 r_m^{-\alpha}$ and $I_{\text{SAT}} = \sum_{j\in\Phi_U} P_{sj} G_{i,j} |h_{pc}^{j}|^2$. Now substituting (c) into (48), the solution yields

$$\begin{aligned}
\mathcal{P}_{\text{out}|\Gamma}^{I}(T_t) &= \frac{\gamma\left(m_{cp}, \frac{\Upsilon m_{cp}}{P_{\text{tot}}}\right)}{\Gamma\left(m_{cp}\right)} \sum_{k=0}^{m_{cc}} \binom{m_{cc}}{k}(-1)^k \\
&\times e^{\frac{-A k r_l^{\alpha} T_t \sigma^2}{P_{\text{tot}}}}\, \mathbb{E}_{I_{\text{BS}}}\left[e^{\frac{-A k r_l^{\alpha} T_t I_{\text{BS}}}{P_{\text{tot}}}}\right] \mathbb{E}_{I_{\text{SAT}}}\left[e^{\frac{-A k r_l^{\alpha} T_t I_{\text{SAT}}}{P_{\text{tot}}}}\right].
\end{aligned} \tag{51}$$

The Laplace transform of terrestrial interference is given as

$$\begin{aligned}
&\mathbb{E}_{I_{\text{BS}}}\left[\exp(-s I_{\text{BS}})\right] \\
&= \mathbb{E}_{I_{\text{BS}}}\left[\prod_{m\in\Phi_{\text{BS}}} \exp\left(-s P_m X_{cc} r_m^{-\alpha}\right)\right], \\
&= \mathbb{E}_{I_{\text{BS}}}\left[\exp\left(-s \sum_{m\in\Phi_{\text{BS}}} P_m X_{cc} r_m^{-\alpha}\right)\right],
\end{aligned} \tag{52}$$

where, $s = \frac{A k r_l^{\alpha} T_t}{P_{\text{tot}}}$ $X_{cc} = |h_{cc}^{m}|^2$.

Applying the Campbell's theorem [40], we obtain[9]

$$\begin{aligned}
&\mathbb{E}_{I_{\Phi_{\text{BS}}}}\left[\exp\left(\frac{-A k r_l^{\alpha} T_t I_{\Phi_{\text{BS}}}}{P_{\text{tot}}}\right)\right] \\
&= \exp\left(-2\pi\lambda_{\text{BS}} \int_r^{\infty}\left(1 - \frac{1}{\left(1+\frac{A k P_m r_l^{\alpha}}{P_{\text{tot}} r^{\alpha}}\right)^{m_{cc}}}\right) r\,\text{dr}\right).
\end{aligned} \tag{53}$$

The expectation of interfering link from the satellite is obtained thus: Let $s = \frac{A k r_l^{\alpha} T_t}{P_{\text{tot}}}$

$$\begin{aligned}
&\mathcal{L}\{I_{\text{SAT}}\}(s) = \mathbb{E}\left[\exp(-s I_{\text{SAT}})\right], \\
&= \mathbb{E}_{\Phi_U, X_{pc}}\left[\prod_{i\in\Phi_U} \exp\left(-s P_{sj} G_{ij} X_{pc}\right)\right], \\
&\overset{(a)}{=} \mathbb{E}_{\Phi_U}\left\{\prod_{i\in\Phi_U} \mathbb{E}_{X_{pc}}\left[\exp\left(-s P_{sj} G_{ij} X_{pc}\right)\right]\right\}, \\
&\overset{(b)}{=} \exp\left[-2\pi\lambda_U\left(1 - \left(\frac{1}{1 + \frac{s P_{sj} G_{ij}}{\beta_s}}\right)^{\alpha_s}\right)\right],
\end{aligned} \tag{54}$$

where $X_{pc} = |h_{pc}^{j}|^2$, (a) follows from the assumption of independent fading, (b) follows from the use of Campbell's theorem, moment generating function of Gamma random variable and probability generating functionals of PPPs.

For the second part of $\mathcal{P}_{\text{out}|\Gamma}$ in (47), we obtain:

$$\mathcal{P}_{\text{out}|\Gamma}^{II}(T_t) = \int_{\frac{\Upsilon}{P_{\text{tot}}}}^{\infty} \underbrace{\mathcal{P}\left[\frac{\frac{\Upsilon}{\Gamma}\ |h_{cc}^{l}|^2 r_l^{-\alpha}}{\sigma^2 + I_{\text{BS}} + I_{\text{SAT}}} < T_t\right]}_{III} f_\Gamma(y)\,\text{dy}, \tag{55}$$

with f_Γ defined in (49). We solve III by following steps similar to those outlined in (50) and obtain

$$\begin{aligned}
&\mathcal{P}\left[\frac{\frac{\Upsilon}{\Gamma}\ |h_{cc}^{l}|^2 r_l^{-\alpha}}{\sigma^2 + I_{\text{BS}} + I_{\text{SAT}}} < T_t\right] = \sum_{k=0}^{m_{cc}} \binom{m_{cc}}{k}(-1)^k e^{\frac{-A k r_l^{\alpha} T_t \Gamma \sigma^2}{\Upsilon}} \\
&\times \prod_{m\in\Phi_{\text{BS}}} \mathbb{E}_{I_{\text{BS}}}\left[e^{-\frac{A k r_l^{\alpha} T_t \Gamma I_{\text{BS}}}{P_{\text{tot}}}}\right] \prod_{j\in\Phi_U} \mathbb{E}_{I_{\text{SAT}}}\left[e^{-\frac{A k r_l^{\alpha} T_t \Gamma I_{\text{SAT}}}{P_{\text{tot}}}}\right].
\end{aligned} \tag{56}$$

[9] r_m is subsequently referred to as r.

Now, substituting (56) into (55), we obtain $\mathcal{P}^{II}_{\text{out}|y}$ given as

$$\mathcal{P}^{II}_{\text{out}|\Gamma}(T_t) = \int_{\frac{\Upsilon}{P_{\text{tot}}}}^{\infty} \sum_{k=0}^{m_{cc}} \binom{m_{cc}}{k} (-1)^k e^{\frac{-A\,k\,r_l^{\alpha}\,T_t\,y\sigma^2}{\Upsilon}} \times \prod_{m\in\Phi_{\text{BS}}} \mathbb{E}_{I_{\text{BS}}}\left[e^{-\frac{-A\,k\,r_l^{\alpha}\,T_t\,y\,I_{\text{BS}}}{P_{\text{tot}}}}\right] \times \prod_{j\in\Phi_U} \mathbb{E}_{I_{\text{SAT}}}\left[e^{-\frac{-A\,k\,r_l^{\alpha}\,T_t\,y I_{\text{SAT}}}{P_{\text{tot}}}}\right] \frac{m_{cp}^{m_{cp}}\, y^{m_{cp}-1}\, e^{-m_{cp}\,y}}{\Gamma(m_{cp})}\,\text{dy}. \quad (57)$$

The expectations of interfering links from the other BSs, $\mathbb{E}_{I_{\text{BS}}}[\exp(-\frac{A\,k\,r_l^{\alpha}\,T_t\,y\,I_{\text{BS}}}{P_{\text{tot}}})]$ and the satellite, $\mathbb{E}_{I_{\text{SAT}}}[\exp(-\frac{A\,k\,r_l^{\alpha}\,T_t\,y\,I_{\text{SAT}}}{P_{\text{tot}}})]$ are obtained by following similar steps to (53) and (54) respectively. Finally, the proof of outage probability for the terrestrial user is realised by summation of $\mathcal{P}^{I}_{\text{out}|y}$ and $\mathcal{P}^{II}_{\text{out}|y}$ respectively.

Appendix B
Proof of Proposition 2

The approximated outage probability for the terrestrial user when $f_{\bar{I}_{\text{BS}}}(x;\nu,\theta) = \frac{x^{\nu-1}e^{-\frac{x}{\theta}}}{\theta^{\nu}\Gamma(\nu)}$ and $I_{\text{SAT}} = 0$ is given as

$$\mathcal{P}_{\text{out}|\Gamma}(T_t) = \underbrace{\int_0^{\frac{\Upsilon}{P_{\text{tot}}}} \mathcal{P}\left[\frac{P_{\text{tot}}\,|h^l_{cc}|^2 r_l^{-\alpha}}{\sigma^2 + I_{\text{BS}}} < T_t\right] f_{\Gamma}(y)\,\text{dy}}_{I} + \underbrace{\int_{\frac{\Upsilon}{P_{\text{tot}}}}^{\infty} \mathcal{P}\left[\frac{\frac{\Upsilon}{\Gamma}\,|h^l_{cc}|^2 r_l^{-\alpha}}{\sigma^2 + I_{\text{BS}}} < T_t\right] f_{\Gamma}(y)\,\text{dy}}_{II}. \quad (58)$$

The expectation of the interfering links from other BSs is given as

$$\mathbb{E}_{I_{\text{BS}}}\left[e^{\left(-\frac{A\,k\,r_l^{\alpha}\,T_t\,I_{\text{BS}}}{P_{\text{tot}}}\right)}\right] = \int_0^{\infty} e^{-\frac{A\,k\,r_l^{\alpha}\,T_t x}{P_{\text{tot}}}} \frac{x^{\nu-1}e^{-\frac{x}{\theta}}}{\theta^{\nu}\Gamma(\nu)}\text{dx}, \quad (59)$$

Solving for (59) yields

$$\mathbb{E}_{I_{\text{BS}}}\left[e^{\left(-\frac{A\,k\,r_l^{\alpha}\,T_t\,I_{\text{BS}}}{P_{\text{tot}}}\right)}\right] = \left(\frac{A\,k\,r_l^{\alpha}\,P_m\,T_t}{P_{\text{tot}}} + \frac{1}{\theta}\right)^{-\nu}\theta^{-\nu}. \quad (60)$$

Using the expressions $\mathbb{E}_{I_{\text{BS}}}\left[e^{\left(-\frac{A\,k\,r_l^{\alpha}\,T_t\,I_{\text{BS}}}{P_{\text{tot}}}\right)}\right]$ and $f_{\Gamma}(y) = e^{-y}$ to solve (58) and following similar steps to Appendix A will yield (29).

Appendix C
Proof of Proposition 3

Now, the outage probability of SINR distribution using (15) can be given as

$$\mathbb{P}\left[\frac{P_{si}G_{ii}|h^i_{pp}|^2}{\sigma^2 + I_{\text{BS}}} < T_s\right] = \mathbb{P}\left[h^i_{pp}|^2 < \frac{T_s}{P_{si}G_{ii}}\left(\sigma^2 + I_{\text{BS}}\right)\right]. \quad (61)$$

Leveraging the tight upper bound of a Gamma random variable of parameters α_s and β_s as $\mathbb{P}[h^i_{pp}|^2 < \gamma < (1-e^{-A\beta_s\gamma})^{\alpha_s}$ with $A = \alpha_s(\alpha_s!)^{\frac{-1}{\alpha_s}}$, and by applying binomial theorem we approximate (61) as

$$\mathbb{P}\left[h^i_{pp}|^2 < \frac{T_s}{P_{si}G_{ii}}\left(\sigma^2 + I_{\text{BS}}\right)\right] \approx \sum_{l=0}^{\alpha_s}\binom{\alpha_s}{l}(-1)^l e^{\frac{-A\,l\,\beta_s\,T_s\sigma^2}{P_{si}G_{ii}}}\mathcal{L}\left\{I_{\Phi_{\text{BS}}}\right\}(s), \quad (62)$$

where $s = \frac{A\,l\,\beta_s\,T_s}{P_{si}G_{ii}}$. Next, the terrestrial interference due to BSs is characterized as

$$\mathcal{L}\left\{I_{\Phi_{\text{BS}}}\right\}(s) = \mathbb{E}_{I_{\Phi_{\text{BS}}}}\left[\exp\left(-s\,I_{\Phi_{\text{BS}}}\right)\right], = \mathbb{E}_{I_{\Phi_{\text{BS}}}}\left[\prod_{l\in\Phi_{\text{BS}}}\exp\left(-s\,P_{\text{ter}}\,|h_{cp}|^2 r_l^{-\alpha}\right)\right], \quad (63)$$

which is gotten by substituting $I_{\Phi_{\text{BS}}} = \sum_{l\in\Phi_{\text{BS}}} P_{\text{ter}}\,|h^i_{cp}|^2\,r_l^{-\alpha}$. Applying Campbell's theorem [40], we obtain

$$\mathcal{L}\{I_{\Phi_{\text{BS}}}\}(s) = \exp\left[2\pi\lambda_{\text{BS}}\int_r^{\infty}\left(e^{-s\,P_{\text{ter}}\,|h^i_{cp}|^2\,r^{-\alpha}} - 1\right)r\text{dr}\right]. \quad (64)$$

Taking the expectation with respect to $|h^i_{cp}|^2$ and recalling that P_{ter} is constrained as in equation (12), we obtain

$$\mathcal{L}\{I_{\Phi_{\text{BS}}}\}(s) = \exp\left[2\pi\lambda_{\text{BS}}\left(\underbrace{\int_r^{\infty}\int_0^{\frac{\Upsilon}{P_{\text{tot}}}}\left(e^{-s\,P_{\text{tot}}\,y\,r^{-\alpha}} - 1\right)f_{\Gamma}(y)\,\text{dy r dr}}_{I} + \underbrace{\int_r^{\infty}\int_{\frac{\Upsilon}{P_{\text{tot}}}}^{\infty}\left(e^{-s\,\frac{\Upsilon}{\Gamma}\,y\,r^{-\alpha}} - 1\right)f_{\Gamma}(y)\,\text{dy r dr}}_{II}\right)\right], \quad (65)$$

where $f_{\Gamma}(y)$ is as defined in (49).

After solving the inner integrals of I and II with respect to y, the expectation of the interference from BSs limited by the interference temperature constraint is given as

$$\mathcal{L}\left\{I_{\Phi_{\text{BS}}}\right\}(s) = \exp\left[2\pi\lambda_{\text{BS}}\left(\int_r^{\infty}\frac{m_{cp}\,\Gamma\left(m_{cp}, \frac{\Upsilon m_{cp}}{P_{\text{tot}}}\right) - \Gamma(m_{cp}+1)}{m_{cp}\Gamma(m_{cp})} + \frac{m_{cp}^{m_{cp}-1}}{\Gamma(m_{cp})}\left(m_{cp} + P_{\text{tot}}r^{-\alpha}s\right)^{-m_{cp}} \times \left(\Gamma\left(m_{cp}+1\right) - m_{cp}\Gamma\left(m_{cp}, \frac{\Upsilon\left(m_{cp}+P_{\text{tot}}r^{-\alpha}s\right)}{P_{\text{tot}}}\right)\right) + \int_r^{\infty}\left(1 - e^{-s\Upsilon r^{-\alpha}}\right)\left(\frac{\gamma\left(m_{cp}, \frac{\Upsilon m_{cp}}{P_{\text{tot}}}\right) - \Gamma\left(m_{cp}\right)}{\Gamma\left(m_{cp}\right)}\right)\right)r\text{dr}\right], \quad (66)$$

where $\Gamma(x, y)$, $\gamma(x, y)$, are the upper and lower incomplete gamma functions respectively, and $\Gamma(x)$ is the gamma function.

This proof is concluded by substituting (66) into (62).

References

[1] D. Tse and P. Viswanath, *Fundamentals of Wireless Communication*. Cambridge, U.K.: Cambridge Univ. Press, 2005.

[2] W. W. Wu, "Satellite communications," *Proc. IEEE*, vol. 85, no. 6, pp. 998–1010, Jun. 1997.

[3] G. Zheng, S. Chatzinotas, and B. Ottersten, "Generic optimization of linear precoding in multibeam satellite systems," *IEEE Trans. Wireless Commun.*, vol. 11, no. 6, pp. 2308–2320, Jun. 2012. AQ4

[4] A. Gharanjik, M. R. B. Shankar, P. D. Arapoglou, M. Bengtsson, and B. Ottersten, "Robust precoding design for multibeam downlink satellite channel with phase uncertainty," in *Proc. ICASSP*, Brisbane, QLD, Australia, 2015, pp. 3083–3087.

[5] L. Cottatellucci *et al.*, "Interference mitigation techniques for broadband satellite systems," in *Proc. ICSSC*, San Diego, CA, USA, 2006. AQ5

[6] S. L. Kota, "Hybrid/integrated networking for NGN services," in *Proc. 2nd Int. Conf. Wireless Commun. Veh. Technol. Inf. Theory Aerosp. Electron. Syst. Technol. (Wireless VITAE)*, Chennai, India, Feb. 2011, pp. 1–6.

[7] S. Morosi, S. Jayousi, and E. D. Re, "Cooperative delay diversity in hybrid satellite/terrestrial DVB-SH system," in *Proc. IEEE ICC*, Cape Town, South Africa, May 2010, pp. 1–5.

[8] N. Devroye, P. Mitran, and V. Tarokh, "Achievable rates in cognitive radio channels," *IEEE Trans. Inf. Theory*, vol. 52, no. 5, pp. 1813–1827, May 2006.

[9] A. Goldsmith, S. A. Jafar, I. Maric, and S. Srinivasa, "Breaking spectrum gridlock with cognitive radios: An information theoretic perspective," *Proc. IEEE*, vol. 97, no. 5, pp. 894–914, May 2009.

[10] Y. Zeng, Y.-C. Liang, A. T. Hoang, and R. Zhang, "A review on spectrum sensing for cognitive radio: Challenges and solutions," *EURASIP J. Appl. Signal Process.*, vol. 2010, Dec. 2010, Art. no. 381465. AQ6

[11] S. K. Sharma, S. Chatzinotas, and B. Ottersten, "Satellite cognitive communications: Interference modeling and techniques selection," in *Proc. 6th Adv. Satellite Multimedia Syst. Conf. (ASMS) 12th Signal Process. Space Commun. Workshop (SPSC)*, Baiona, Spain, Sep. 2012, pp. 111–118.

[12] S. Kandeepan, L. D. Nardis, M.-G. D. Benedetto, A. Guidotti, and G. E. Corazza, "Cognitive satellite terrestrial radios," in *Proc. IEEE GLOBECOM*, Miami, FL, USA, Dec. 2010, pp. 1–6.

[13] S. K. Sharma, S. Chatzinotas, and B. Ottersten, "Cognitive radio techniques for satellite communication systems," in *Proc. IEEE VTC*, Las Vegas, NV, USA, Sep. 2013, pp. 1–5.

[14] S. Vassaki, M. I. Poulakis, A. D. Panagopoulos, and P. Constantinou, "Power allocation in cognitive satellite terrestrial networks with QoS constraints," *IEEE Commun. Lett.*, vol. 17, no. 7, pp. 1344–1347, Jul. 2013.

[15] E. Lagunas, S. K. Sharma, S. Maleki, S. Chatzinotas, and B. Ottersten, "Resource allocation for cognitive satellite communications with incumbent terrestrial networks," *IEEE Trans. Cogn. Commun. Netw.*, vol. 1, no. 3, pp. 305–317, Sep. 2015.

[16] K. An, M. Lin, W.-P. Zhu, Y. Huang, and G. Zheng, "Outage performance of cognitive hybrid satellite–terrestrial networks with interference constraint," *IEEE Trans. Veh. Technol.*, vol. 65, no. 11, pp. 9397–9404, Nov. 2016.

[17] A. Gharanjik, M. R. B. Shankar, P.-D. Arapoglou, M. Bengtsson, and B. Ottersten, "Precoding design and user selection for multibeam satellite channels," in *Proc. IEEE 16th Int. Workshop Signal Process. Adv. Wireless Commun. (SPAWC)*, Stockholm, Sweden, Jun. 2015, pp. 420–424.

[18] C.-H. Lee and M. Haenggi, "Interference and outage in poisson cognitive networks," *IEEE Trans. Wireless Commun.*, vol. 11, no. 4, pp. 1392–1401, Apr. 2012.

[19] H. ElSawy, E. Hossain, and M. Haenggi, "Stochastic geometry for modeling, analysis, and design of multi-tier and cognitive cellular wireless networks: A survey," *IEEE Commun. Surveys Tuts.*, vol. 15, no. 3, pp. 996–1019, 3rd Quart., 2013.

[20] R. Ramanathan, J. Redi, C. Santivanez, D. Wiggins, and S. Polit, "Ad hoc networking with directional antennas: A complete system solution," *IEEE J. Sel. Areas Commun.*, vol. 23, no. 3, pp. 496–506, Mar. 2005.

[21] H. Wang and M. C. Reed, "Tractable model for heterogeneous cellular networks with directional antennas," in *Proc. Aust. Commun. Theory Workshop (AusCTW)*, Wellington, New Zealand, Jan. 2012, pp. 61–65.

[22] S. K. Sharma, S. Chatzinotas, and B. Ottersten, "Transmit beamforming for spectral coexistence of satellite and terrestrial networks," in *Proc. 8th Int. Conf. Cogn. Radio Orient. Wireless Netw.*, Washington, DC, USA, Jul. 2013, pp. 275–281.

[23] G. Zheng, S. Chatzinotas, and B. Ottersten, "Multi-gateway cooperation in multibeam satellite systems," in *Proc. PIMRC*, Sydney, NSW, Australia, Sep. 2012, pp. 1360–1364.

[24] D. Christopoulos, S. Chatzinotas, and B. Ottersten, "Multicast multigroup precoding and user scheduling for frame-based satellite communications," *IEEE Trans. Wireless Commun.*, vol. 14, no. 9, pp. 4695–4707, Sep. 2015.

[25] G. Taricco, "Linear precoding methods for multi-beam broadband satellite systems," in *Proc. 20th Eur. Wireless Conf.*, Barcelona, Spain, May 2014, pp. 1–6.

[26] M. A. Vazquez *et al.*, "Precoding in multibeam satellite communications: Present and future challenges," *IEEE Wireless Commun.*, vol. 23, no. 6, pp. 88–95, Dec. 2016.

[27] A. Abdi, W. C. Lau, M.-S. Alouini, and M. Kaveh, "A new simple model for land mobile satellite channels: First-and second-order statistics," *IEEE Trans. Wireless Commun.*, vol. 2, no. 3, pp. 519–528, May 2003.

[28] B. Vucetic and J. Du, "Channel modeling and simulation in satellite mobile communication systems," *IEEE J. Sel. Areas Commun.*, vol. 10, no. 8, pp. 1209–1218, Oct. 1992.

[29] G. Fraidenraich, O. Leveque, and J. M. Cioffi, "On the MIMO channel capacity for the Nakagami-*m* channel," in *Proc. IEEE GLOBECOM*, Washington, DC, USA, 2007, pp. 3612–3616.

[30] M. Haenggi, "A geometric interpretation of fading in wireless networks: Theory and applications," *IEEE Trans. Inf. Theory*, vol. 54, no. 12, pp. 5500–5510, Dec. 2008.

[31] C. Psomas, M. Mohammadi, I. Krikidis, and H. A. Suraweera, "Impact of directionality on interference mitigation in full-duplex cellular networks," *IEEE Trans. Wireless Commun.*, vol. 16, no. 1, pp. 487–502, Jan. 2017.

[32] A. M. Hunter, J. G. Andrews, and S. Weber, "Transmission capacity of ad hoc networks with spatial diversity," *IEEE Trans. Wireless Commun.*, vol. 7, no. 12, pp. 5058–5071, Dec. 2008.

[33] B. R. Vojcic and W. M. Jang, "Transmitter precoding in synchronous multiuser communications," *IEEE Trans. Commun.*, vol. 46, no. 10, pp. 1346–1355, Oct. 1998.

[34] Y. S. Soh, T. Q. S. Quek, M. Kountouris, and H. Shin, "Energy efficient heterogeneous cellular networks," *IEEE J. Sel. Areas Commun.*, vol. 31, no. 5, pp. 840–850, May 2013.

[35] A. Rabbachin, T. Q. S. Quek, H. Shin, and M. Z. Win, "Cognitive network interference," *IEEE J. Sel. Areas Commun.*, vol. 29, no. 2, pp. 480–493, Feb. 2011.

[36] A. Ghasemi and E. S. Sousa, "Interference aggregation in spectrum-sensing cognitive wireless networks," *IEEE J. Sel. Topics Signal Process.*, vol. 2, no. 1, pp. 41–56, Feb. 2008.

[37] R. W. Heath, M. Kountouris, and T. Bai, "Modeling heterogeneous network interference using Poisson point processes," *IEEE Trans. Signal Process.*, vol. 61, no. 16, pp. 4114–4126, Aug. 2013.

[38] N. Valliappan, A. Lozano, and R. W. Heath, "Antenna subset modulation for secure millimeter-wave wireless communication," *IEEE Trans. Commun.*, vol. 61, no. 8, pp. 3231–3245, Aug. 2013.

[39] A. Adhikary *et al.*, "Joint spatial division and multiplexing for mm-wave channels," *IEEE J. Sel. Areas Commun.*, vol. 32, no. 6, pp. 1239–1255, Jun. 2014.

[40] M. Haenggi, *Stochastic Geometry for Wireless Networks*. Cambridge, U.K.: Cambridge Univ. Press, 2012.

[41] H. ElSawy and E. Hossain, "A modified hard core point process for analysis of random CSMA wireless networks in general fading environments," *IEEE Trans. Commun.*, vol. 61, no. 4, pp. 1520–1534, Apr. 2013.

[42] H. Q. Nguyen, F. Baccelli, and D. Kofman, "A stochastic geometry analysis of dense IEEE 802.11 networks," in *Proc. IEEE ICC*, Barcelona, Spain, 2007, pp. 1199–1207.

[43] A. Papoulis and S. U. Pillai, *Probability, Random Variables, and Stochastic Processes*. Boston, MA, USA: McGraw-Hill, 2002.

Oluwatayo Y. Kolawole (S'15) received the B.Eng. degree (Hons.) in electrical electronics engineering from Abubakar Tafawa Balewa University, Nigeria, in 2010 and the M.Sc. degree in signal processing and communications from the University of Edinburgh in 2014, where she is currently pursuing the Ph.D. degree with the Institute for Digital Communications. Her main area of research is wireless communications, with particular focus on millimeter wave and stochastic geometry.

Satyanarayana Vuppala (S'12–M'17) received the B.Tech. degree (with Distinction) in computer science and engineering from JNTU, Kakinada, India, in 2009, the M.Tech. degree in information technology from the National Institute of Technology, Durgapur, India, in 2011, and the Ph.D. degree in electrical engineering from Jacobs University Bremen, in 2014. He is currently a Post-Doctoral Researcher with the Interdisciplinary Centre for Security, Reliability and Trust, University of Luxembourg. His main research interests are physical, access, and network layer aspects of wireless security. He also works on performance evaluation of mmWave systems. He was a recipient of MHRD, India Scholarship from 2009 to 2011.

Mathini Sellathurai (SM'XX) is a Full Professor of signal processing and intelligent systems with Heriot-Watt University, Edinburgh, U.K. In her 15-year research on Signal Processing for Communications, she has made seminal contributions on MIMO wireless systems. She has published 200 IEEE entries with over 2300 citations, given invited talks and has written a book and several book chapters in topics related to this project. She was a recipient of the IEEE Communication Society Fred W. Ellersick Best Paper Award in 2005, the Industry Canada Public Service Awards for contributions in science and technology in 2005, and the Best Ph.D. Thesis Award (Silver Medal) from NSERC Canada in 2002. She is also a member for IEEE SPCOM Technical Strategy Committee, an Editor of IEEE TSP from 2009 to 2014, since 2015. She is also the General Co-Chair of IEEE SPAWC2016 in Edinburgh. She is a fellow of Higher Education Academy, U.K.

AQ7

Tharmalingam Ratnarajah (A'96–M'05–SM'05) is currently with the Institute for Digital Communications (IDCOM), University of Edinburgh, Edinburgh, U.K., as the Head of IDCOM and a Professor of digital communications and signal processing. He was the Coordinator of FP7 Future and Emerging Technologies project CROWN (2.3M€) in the area of cognitive radio networks and HIATUS (2.7M€) in the area of interference alignment. He is currently the Coordinator of the FP7 projects HARP (3.2M€) in the area of highly distributed MIMO and ADEL (3.7M€) in the area of licensed shared access. He has published over 300 publications in the above areas and holds four U.S. patents. His research interests include signal processing and information theoretic aspects of 5G wireless networks, full-duplex radio, mmWave communications, random matrices theory, interference alignment, statistical and array signal processing, and quantum information theory. He is a fellow of Higher Education Academy, U.K.

AUTHOR QUERIES

AUTHOR PLEASE ANSWER ALL QUERIES

PLEASE NOTE: We cannot accept new source files as corrections for your paper. If possible, please annotate the PDF proof we have sent you with your corrections and upload it via the Author Gateway. Alternatively, you may send us your corrections in list format. You may also upload revised graphics via the Author Gateway.

AQ1: Please confirm/give details of funding source.

AQ2: Please be advised that per instructions from the Communications Society this proof was formatted in Times Roman font and therefore some of the fonts will appear different from the fonts in your originally submitted manuscript. For instance, the math calligraphy font may appear different due to usage of the usepackage[mathcal]euscript. The Communications Society has decided not to use Computer Modern fonts in their publications.

AQ3: Note that if you require corrections/changes to tables or figures, you must supply the revised files, as these items are not edited for you.

AQ4: References [3] and [28] were the same, so Reference [28] has been deleted, and the following references (and their in text citations) have been renumbered. Please check and confirm that they are correct as set.

AQ5: Please provide the page range for Reference [5].

AQ6: Please confirm the volume number for Reference [10].

AQ7: Please provide the missing IEEE membership year for the author "M. Sellathurai."